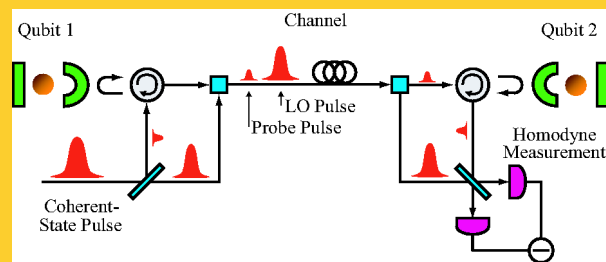


Abstract This article reviews recent hybrid approaches to optical quantum information processing, in which both discrete and continuous degrees of freedom are exploited. There are well-known limitations to optical single-photon-based qubit and multi-photon-based qumode implementations of quantum communication and quantum computation, when the toolbox is restricted to the most practical set of linear operations and resources such as linear optics and Gaussian operations and states. The recent hybrid approaches aim at pushing the feasibility, the efficiencies, and the fidelities of the linear schemes to the limits, potentially adding weak or measurement-induced nonlinearities to the toolbox.



Schematics for the optical implementation of entanglement distribution between two stations in a hybrid quantum repeater.

Copyright line will be provided by the publisher

Optical hybrid approaches to quantum information

Peter van Loock

Optical Quantum Information Theory Group, Max Planck Institute for the Science of Light,
Institute of Theoretical Physics I, Universität Erlangen-Nürnberg, Staudstr.7/B2, 91058 Erlangen, Germany

Received: ...

Published online: ...

Key words: quantum computation, quantum communication, quantum optics, entanglement, qubits, qumodes, hybrid

Contents

1. Introduction	1
2. Optical quantum information	3
3. Hybrid approaches	13
4. Summary and outlook	31

1. Introduction

Quantum information is a relatively young area of interdisciplinary research. One of its main goals is, from a more conceptual point of view, to combine the principles of quantum physics with those of information theory. Information is physical is one of the key messages, and, on a deeper level, it is quantum physical. Apart from its conceptual importance, however, quantum information may also lead to real-world applications for communication (quantum communication) and computation (quantum computation) by exploiting quantum properties such as the superposition principle and entanglement. In recent years, especially entanglement turned out to play the most prominent role, representing a universal resource for both quantum computa-

tion and quantum communication. More precisely, multipartite entangled, so-called cluster states are a sufficient resource for universal, measurement-based quantum computation [1]. Further, the sequential distribution of many copies of entangled states in a quantum repeater allow for extending quantum communication to large distances, even when the physical quantum channel is imperfect such as a lossy, optical fiber [2,3].

Many if not most experiments related to quantum information are conducted with quantum optical systems. This includes the preparation, manipulation, and measurement of interesting and useful quantum optical states, in particular, entangled states; possibly supplemented by additional atomic systems for storing and processing quantum states.

Why is quantum optics the preferred field for quantum information demonstrations? Based on mature techniques from nonlinear optics for state preparation such as parametric down conversion, together with the most accessible means for manipulating optical states with linear elements such as beam splitters, there is a long list of optical proof-of-principle demonstrations of various quantum information processing tasks. Some of these experi-

ments are performed with single-photon states, leading to a *discrete-variable* (DV) encoding of quantum information, where, for instance, a qubit space is spanned by two orthogonal polarizations ('photonic qubits') [4]. In other experiments, *continuous-variable* (CV) states, defined in an infinite-dimensional Hilbert space, are utilized, for example, expressed in terms of the quadrature amplitudes of an optical, bosonic mode ('photonic qumodes') [5]. Typically, the DV experiments involve some heralding mechanism, rendering them conditional, and hence less efficient; nonetheless, fidelities in the DV schemes are fairly high [6]. Conversely, in the CV regime, unconditional operations and high efficiencies are at the expense of lower fidelities [7].

Beyond experimental small-scale demonstrations, towards potential real-world applications, light is clearly the optimal choice for communication. Moreover, in order to mediate interactions between distant matter qubits on a fixed array (for instance, in a solid-state system), individual photons or intense light pulses may be utilized. In such a scenario, the light field acts as a kind of quantum bus ('qubus') for applying entangling gates to the matter qubits. This kind of optical, qubus-mediated quantum logic could become part of a full quantum computer. In addition, it is exactly this qubus approach which can be exploited for quantum communication in a quantum repeater, where the optical qubus propagates through a fiber (or even through free space) between neighboring repeater stations and locally interacts with each matter qubit for nonlocal, entangled-state preparation of the two distant qubits. In analogy to classical, optical/electronic hybrid computers, the above schemes may be referred to as '*hybrid*' approaches, as they combine the useful features of both light and matter; the former as an ideal medium for communicating, the latter well suited for storing quantum information.

In addition to the hybrid notion mentioned in the preceding paragraph, there is a related, but somewhat different definition of (optical) hybrid quantum information protocols. These are inspired by practical as well as fundamental limitations of those optical quantum information schemes, which are solely based upon either discrete or continuous degrees of freedom. A hybrid scheme, similar to a classical, digital/analog hybrid computer, would then exploit at the same time both DV and CV states, encodings, gates, measurements, and techniques, in order to circumvent those limitations.

1.1. CV versus DV

It is well known that a very strong version of universal quantum computation ('CV universality'), namely the ability to simulate any Hamiltonian, expressed as an arbitrary polynomial of the bosonic mode operators, to arbitrary precision, is not achievable with only linear transformations, i.e., Gaussian transformations [8]. Gaussian transformations are rotations and translations in phase space, as well

as beam splitting and squeezing unitaries, all transforming Gaussian states into Gaussian states. Similarly, a fully Gaussian qumode quantum computer can always be efficiently simulated by a classical computer [9]. A single non-Gaussian element such as a cubic Hamiltonian would be sufficient to both achieve universality and prevent classical simulability. In general, however, non-Gaussian transformations are difficult to realize on optical Gaussian states; nonetheless deterministic protocols for approximating such gates exist [10] (the 'GKP' scheme).

Although the physical states in quantum optical approaches, representing quantized harmonic oscillators, would always live in infinite-dimensional Fock space, there is a weaker, but possibly more useful notion of universality ('DV universality'). It refers to the ability to approximately simulate any DV multi-qubit unitary with a finite set of gates, logically acting on a finite subspace of the infinite-dimensional optical Fock space, spanned by states with only a few photons (photonic qubits). In this case, a universal set must also contain a nonlinear interaction, unless we accept probabilistic operations [11] (the 'KLM' scheme). Similarly, exactly fulfilling finite tasks supposedly simpler than universal quantum computation, such as a complete, photonic two-qubit Bell measurement, would be impossible with only linear elements (including squeezers) [12, 13, 14]. The problem is that nonlinear interactions on the level of single photons are hard to obtain. It is very difficult to make two photons "talk" to each other.

1.2. Going hybrid

In a hybrid scheme, where DV and CV degrees of freedom are exploited at the same time and the goal is to circumvent the limitations of the linear approaches, it can be useful to consider two special notions of nonlinearity: one is that of weak nonlinearities, the other one is that of measurement-induced nonlinearities. The former one would then be effectively enhanced through the use of sufficiently intense light fields; an approach first utilized for quantum non-demolition measurements with CV states [15]. More recently, weak nonlinearities were applied to combined DV-CV, i.e., hybrid systems, where the weak nonlinear interaction is not only enhanced, but also mediated between the DV components through a bright CV qubus state. This enables one to perform various tasks from projecting onto the complete, photonic DV Bell basis to implementing universal, photonic two-qubit entangling gates, using either DV (threshold) photon detectors [16], CV homodyne detectors [17, 18, 19, 20], or no detectors at all [21, 22].

The concept of a measurement-induced nonlinearity was initiated by the seminal works of KLM [11] and GKP [10]. The KLM protocol is a fully DV scheme, using complicated, entangled, multi-photon ancilla states, measurements of photon number, and feedforward, whereas the GKP scheme may be considered one of the first hybrid protocols. It relies upon DV photon number measurements, to create non-Gaussian states from CV Gaussian resources,

and to eventually realize non-Gaussian (cubic) CV gates. The GKP proposal also contains the hybrid concept of encoding logical DV states into physical CV states.

At this point, before going into more detail in the following sections, let us summarize the key elements of the optical hybrid approaches to quantum information processing reviewed in this article. The goal of circumventing the limitations of the most practical, linear optical schemes, maintaining to some extent their feasibility and efficiency, and still achieving a true quantum advantage over classical schemes may be reached through all or some of the following ingredients:

- hybrid states and operations, i.e., a combination of DV and CV elements,
- qubus systems for mediating entangling gates,
- weak nonlinearities,
- measurement-induced nonlinearities.

The paper is organized as follows. In Section 2, we give a brief introduction to optical quantum information. This includes a description of how to encode quantum information into photonic qubits and qumodes, how to process such quantum information using linear and nonlinear transformations, and how these tools may be exploited to achieve (theoretically and experimentally) efficient (scalable?) quantum computation and communication. Section 3 then presents the concept of optical hybrid protocols, discussing various hybrid schemes for both quantum computation and communication. Finally, we summarize and conclude in Section 4.

2. Optical quantum information

How can we encode quantum information, for instance, a qubit, into optical states? Do quantum optical states naturally allow for different types of encoding? These questions, together with the issue of processing quantum information encoded in optical states in an efficient way, will be addressed in this section. In particular, we discuss that there are qualitatively different levels of ‘efficient’ optical quantum information processing. These depend on the type of encoding, and on the scalability and the feasibility of the optical resources necessary for their implementation.

2.1. Linear versus nonlinear operations

In Fig. 2.1.1, a table is shown summarizing possible optical interactions and transformations for state preparation and manipulation.

The most accessible and practical interactions are those described by linear and quadratic Hamiltonians. Here, quadratic refers to the order of a polynomial of the mode operators \hat{a}_k for the modes that participate in the interaction.

Each \hat{a}_k (\hat{a}_k^\dagger) corresponds to the annihilation/lowering (creation/raising) operator of a quantized harmonic oscillator, each representing a single mode from a discrete set of (spatial, frequency, polarization, etc.) modes into which the electromagnetic field is most conveniently expanded [23].

	unitary transformation	interaction (Hamiltonian)	input-output relation of mode operators
Gaussian	displacement in phase space	linear	“scalar”
	beam splitter	quadratic	linear
	squeezing	quadratic	linear
	non-Gaussian (cubic phase gate, Kerr effect)	cubic or higher	nonlinear

linear, nonlinear optical interactions

Figure 2.1.1 Optical interactions and transformations in terms of the annihilation and creation operators representing a discrete set of modes of the optical field.

The unitary transformations generated from quadratic Hamiltonians are linear. An arbitrary quadratic Hamiltonian transforms the mode operators as

$$\hat{a}'_k = \sum_l A_{kl} \hat{a}_l + B_{kl} \hat{a}_l^\dagger + \gamma_l. \quad (1)$$

Here, the matrices A and B satisfy the conditions $AB^T = (AB^T)^T$ and $AA^\dagger = BB^\dagger + \mathbb{1}$ according to the bosonic commutation relations $[\hat{a}'_k, \hat{a}'_l^\dagger] = [\hat{a}_k, \hat{a}_l^\dagger] = \delta_{kl}$. This transformation is also referred to as linear unitary Bogoliubov transformation (LUBO) [24]. It combines passive and active elements, i.e., beam splitters and squeezers, respectively; the γ_l 's in Eq. (1) describe phase-space displacements and come from the linear terms in the Hamiltonian. As an example, in a single-mode squeezer, $\hat{a}' = \hat{a} \cosh r - \hat{a}^\dagger \sinh r$, the x -quadrature would be ‘squeezed’, $\hat{x}' = e^{-r} \hat{x}$, and the p -quadrature correspondingly ‘anti-squeezed’, $\hat{p}' = e^{+r} \hat{p}$, with $\hat{a} = \hat{x} + i\hat{p}$ and $\hat{a}' = \hat{x}' + i\hat{p}'$. The quadratures here are dimensionless variables playing the roles of position and momentum with $[\hat{x}, \hat{p}] = i/2$.

Comparing the LUBO to a purely passive (photon number preserving), linear transformation,

$$\hat{a}'_k = \sum_l U_{kl} \hat{a}_l, \quad (2)$$

with an arbitrary unitary matrix U , we observe that there is no mixing between the annihilation and creation operators in the passive transformation. Despite this difference, also the active, more general LUBO is only linear in the mode operators. Therefore, general linear optical transformations are here referred to as LUBOs, including squeezers. As squeezing, however, typically involves a nonlinear optical interaction (such as $\chi^{(2)}$)¹, it may as well be excluded from the ‘linear-optics’ toolbox (see Fig. 2.1.1).

¹ for which the actual, fully quantum mechanical Hamiltonian is cubic; with the usual parametric approximation, considering

Initially, squeezing was not really considered a useful tool for DV quantum information processing. Moreover, it is hard to apply squeezing to an arbitrary state such as a photonic qubit (see next section) ‘online’ in a controlled and efficient way. Hence, usually, squeezing will be explicitly excluded from the linear-optics toolbox for DV quantum information [6, 11]. In the CV approaches, however, optical squeezed states are the essential resource for creating Gaussian CV entangled states [7]. In this case, squeezed states are first created ‘offline’ and then linearly transformed, according to the passive transformation in Eq. (2). In more recent experiments, it was demonstrated that even online squeezing may be shifted offline using squeezed ancilla states [25, 26, 27]. Only these very new approaches would allow for efficient online squeezing of photonic DV states, as potentially needed in hybrid schemes.

In the hybrid context, and in the view of the recent offline-squeezing experiments [25, 26, 27], it is sensible to define the complete set of *linear resources and operations* as all offline prepared, optical Gaussian states and all general LUBOs which are equivalent to Gaussian transformations mapping a Gaussian state back to a Gaussian state, see Fig. 2.1.1. Particularly practical resources here are coherent states, as these are readily and directly available from a laser source. To these coherent-state sources, we then add deterministic, online squeezing, and as a Gaussian, linear measurement, homodyne detection.

The link between the elementary quantum optical devices such as phase shifters, beam splitters, and single-mode squeezers on one side and an arbitrary LUBO as in Eq. (1) on the other side is provided through two important results:

- any active, multi-mode LUBO as in Eq. (1) can be decomposed into a three-step circuit consisting of a passive, linear optical multi-mode transformation, single-mode squeezers, and another passive, linear optical multi-mode transformation [28]
- any passive, linear optical multi-mode transformation described by an arbitrary unitary matrix as in Eq. (2) can be realized through a sequence of two-mode beam splitters and single-mode phase shifters [29]

The former result, the so-called ‘Bloch-Messiah reduction’, can be derived through singular value decomposition, with $A = UA_DV^\dagger$ and $B = UB_DV^T$, a pair of unitary matrices U and V , and non-negative diagonal matrices A_D and B_D , $A_D^2 = B_D^2 + \mathbb{1}$ [28]. The two results together imply that any multi-mode LUBO, i.e., any linear multi-mode transformation as in Eq. (1), can be implemented with single-mode phase shifters, single-mode squeezers, and two-mode beam splitters. The displacements in Eq. (1) (the γ_i ’s) can be also realized using highly reflective beam splitters.

the so-called pump field classical, the pump mode operator becomes a complex number which is then absorbed into the squeezing parameter of the resulting quadratic Hamiltonian.

As shown in Fig. 2.1.1, going beyond the regime of linear resources and operations means to include cubic or higher-order interactions leading to nonlinear transformations. Such a nonlinear interaction would normally map a Gaussian state onto a non-Gaussian state, described by non-Gaussian Q and Wigner functions, see Fig. 2.1.2. These interactions are typically very weak; an example would be the extremely weak Kerr effect in an optical fiber. Therefore, for sufficiently long interaction times, unwanted photon losses will normally dominate over the desired nonlinear transformation.

Rather than performing nonlinear transformations online, we may first create offline nonlinear resources [10, 11] such as photon number (Fock) states as well as other non-Gaussian states such as ‘cat states’ (i.e., superposition states of coherent states, see Fig. 2.1.2 on the right). Typically, this offline preparation would be probabilistic, i.e., conditional, depending on, for instance, certain photon number measurement outcomes for a subset of modes [30, 31, 32].

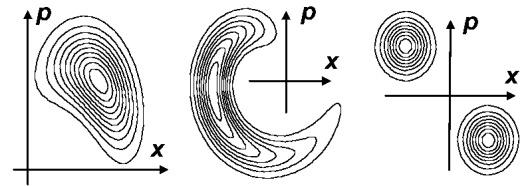


Figure: 2.1.2 Examples of single-mode states generated through highly nonlinear interactions. Shown is the Q function $Q(x, p)$ for a Gaussian coherent state evolving into various non-Gaussian states subject to a quartic self-Kerr interaction with $\hat{H} \propto \hat{a}^\dagger \hat{a} (\hat{a}^\dagger \hat{a} - 1)$.

Let us now explicitly consider the encoding and processing of quantum information using optical resources and linear/nonlinear optical transformations.

2.2. Qubits versus qumodes

The information being processed through a quantum computer is most commonly represented by a set of two-level systems (qubits), in analogy to classical, digital bit encoding. These qubit states could be superpositions of two different, electronic spin projections, or, in the optical context, superpositions of two orthogonal polarizations. As the bosonic Fock space is infinite-dimensional, however, there is much more room for encoding quantum information into optical states. Allowing for states with more than a single photon per mode is a possible way to represent multi-level systems. Alternatively, a multi-level state can be expressed through sufficiently many modes with at most one photon in total.

Apart from discrete photon numbers, an optical state may be described by its amplitude and phase. The corresponding quantum phase-space variables could be considered the quantum analogues of classical, analog encoding. Such phase-space representations would completely determine the state of a quantized optical mode (qumode).

2.2.1. Photonic qubits

Consider the free electromagnetic field with a Hamiltonian $\hat{H} = \sum_k \hbar\omega_k (\hat{a}_k^\dagger \hat{a}_k + 1/2)$ with photon number operator $\hat{a}_k^\dagger \hat{a}_k$ for mode k . Note that the sum includes the zero-point energy '1/2' for every mode. Then the number (Fock) states $|n_k\rangle$, eigenstates of $\hat{a}_k^\dagger \hat{a}_k$, form a complete, orthogonal basis for each mode. Dropping the mode index, we have the well-known relations for annihilating and creating photons, $\hat{a}|n\rangle = \sqrt{n}|n-1\rangle$ and $\hat{a}^\dagger|n\rangle = \sqrt{n+1}|n+1\rangle$, respectively. The vacuum state, containing no photons, is defined as $\hat{a}|0\rangle = 0$.

Using this number basis, there are now (at least) two different ways to encode an optical qubit. The first encoding is called 'single-rail' (or 'occupation number'), as it relies upon just a single optical mode,

$$\cos(\theta/2)|0\rangle + e^{i\phi} \sin(\theta/2)|1\rangle. \quad (3)$$

This encoding, however, is rather inconvenient, because even simple single-qubit rotations would require nonlinear interactions. For example, the Hadamard gate, acting as $|k\rangle \rightarrow (|0\rangle + (-1)^k|1\rangle)/\sqrt{2}$, transforms a Gaussian state (the vacuum) into a non-Gaussian state (a superposition of vacuum and one-photon Fock state).

In contrast, for the so-called 'dual-rail' encoding,

$$\cos(\theta/2)|10\rangle + e^{i\phi} \sin(\theta/2)|01\rangle, \quad (4)$$

single-qubit rotations become an easy task (see Fig. 2.2.1). A 50:50 beam splitter, for instance, would turn $|10\rangle = \hat{a}_1^\dagger|00\rangle$ into $(1/\sqrt{2})(\hat{a}_1^\dagger + \hat{a}_2^\dagger)|00\rangle = (1/\sqrt{2})(|10\rangle + |01\rangle)$, and similarly for the other basis state. The linear transformation here is a simple, special case of the general passive transformation in Eq. (2), and the two modes are spatial.

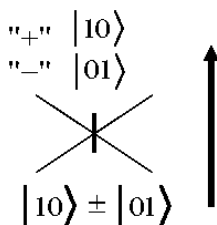


Figure 2.2.1 Using a beam splitter to switch between the computational and the Hadamard transformed, conjugate basis. Here, measuring the photons at the output of the beam splitter would project the input state onto the conjugate basis.

The most common dual-rail encoded, photonic qubit is a polarization encoded qubit,

$$\cos(\theta/2)|H\rangle + e^{i\phi} \sin(\theta/2)|V\rangle, \quad (5)$$

for two polarization modes, where one is horizontally, the other one vertically polarized. So polarization encoding is by no means different from dual-rail encoding; it is rather a specific manifestation of dual-rail encoding. Single-qubit rotations are then particularly simple, corresponding to polarization rotations.

The drawback of the dual-rail encoding is that for realizing two-qubit entangling gates, it is necessary to make two photons (each representing a dual-rail qubit) 'talk' to each other. This kind of interaction between two photons would require some form of nonlinearity. Later we will discuss various possibilities for such two-photon entangling gates. We will also discuss an extension of dual-rail to multiple-rail encoding, where every logical basis state is represented by a single photon that can occupy any one of sufficiently many, different modes (not just two as for dual-rail encoding).

Towards photonic qubit processing, the most accessible, optical resources and their optical manipulation can be summarized as follows.

Resources: single-photon states (i.e., conditionally prepared Fock states, superpositions of Fock states), producible through $\chi^{(2)}$ nonlinear interactions (i.e., parametric down conversion); polarization-encoded states; single-photon states approximated by weak coherent states.

Processing: passive linear optics (beam splitters, phase shifters, polarization rotators).

Measurements: photon counting; on/off detectors.

However, creating a Fock state with many photons is hard, as well as counting large photon numbers. For this purpose, the on/off detector is more realistic, as it does not discriminate between different photon numbers, but only between the vacuum state ('no click') and the non-vacuum state ('click').

For efficiently generating and measuring states with many photons, it is more practical to enter the regime of Gaussian states with CV homodyne detections (see next section). We may further add squeezing to the above toolbox. The truly nonlinear regime for processing is attainable by including, for instance, measurement-induced nonlinearities plus feedforward operations [11].

Despite the difficulty for realizing a two-photon entangling gate, there is a clear advantage of the single-photon encoding. Single photons are fairly robust against noise. Therefore, typically, processing single-photon states can be achieved with high fidelity, though, in most cases, only conditional operations are possible, at potentially very low success probabilities. As extra resources for processing DV quantum information, the atomic counterpart of the photonic polarization (spin) states are the electronic spin states whose qubit representations we shall introduce and utilize later.

We will now introduce a kind of complementary way to encode quantum information, in terms of qumodes. This

type of encoding leads to states which are rather sensitive to noise, but which can be processed in an unconditional fashion; even entangling gates can be achieved through deterministic, linear optics.

2.2.2. Photonic qumodes

Consider again the free electromagnetic field with a Hamiltonian $\hat{H} = \sum_k \hbar\omega_k(\hat{a}_k^\dagger\hat{a}_k + 1/2)$ with photon number operator $\hat{a}_k^\dagger\hat{a}_k$ for mode k . This time we shall rewrite the Hamiltonian as $\hat{H} = \sum_k(\hat{p}_k^2 + \omega_k^2\hat{x}_k^2)/2$, with the position and momentum operators $\hat{x}_k = \sqrt{\hbar/2\omega_k}(\hat{a}_k + \hat{a}_k^\dagger)$ and $\hat{p}_k = -i\sqrt{\hbar\omega_k/2}(\hat{a}_k - \hat{a}_k^\dagger)$ for each oscillator (mode) k . The zero-point energy ‘1/2’ is still present and becomes manifest in the vacuum fluctuations of the position and momentum of every mode.

Further, we have the commutators $[\hat{a}_k, \hat{a}_l^\dagger] = \delta_{kl}$ and $[\hat{x}_k, \hat{p}_l] = i\hbar\delta_{kl}$. After rescaling \hat{x}_k and \hat{p}_k into dimensionless variables, we arrive at $\hat{a}_k = \hat{x}_k + i\hat{p}_k$ with $[\hat{x}_k, \hat{p}_l] = i\delta_{kl}/2$, corresponding to $\hbar = 1/2$, as before. The position and momentum (quadrature) eigenstates may serve as a CV basis to represent the infinite-dimensional state of an optical qumode.

The vacuum state can now be written, for example, in the position basis, $|0\rangle = \int dx \psi_0(x)|x\rangle_x$, with the wave function $\psi_0(x) = (2/\pi)^{1/4} \exp(-x^2)$. It must not be confused with the (unphysical, unnormalized) zero-position eigenstate $|x=0\rangle_x$. The position probability distribution of the vacuum state is a normalized Gaussian, $|\psi_0(x)|^2 = \sqrt{2/\pi} \exp(-2x^2)$. The first and second moments of the vacuum state are easily calculated as (dropping the mode index) $\langle 0|\hat{x}|0\rangle = 0$ and $\langle 0|\hat{x}^2|0\rangle = 1/4$, and similarly for the momentum. Thus, the quadrature vacuum variances are $1/4$. The Wigner function of the vacuum state is $W(x, p) = (2/\pi) \exp[-2(x-x_0)^2 - 2(p-p_0)^2]$, with $x_0 = p_0 = 0$. For finite x_0 and p_0 , with $\alpha = x_0 + ip_0$, we obtain the Wigner function for a displaced vacuum, i.e., a coherent state $|\alpha\rangle$.

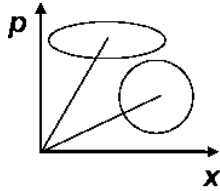


Figure: 2.2.2 Encoding of qumodes into CV Gaussian squeezed and coherent states. Largely squeezed states would approximately resemble position or momentum eigenstates.

The coherent state is also the eigenstate of the non-Hermitian annihilation operator, $\hat{a}|\alpha\rangle = \alpha|\alpha\rangle$, with, correspondingly, complex eigenvalues α . Its mean photon number is therefore $\langle \alpha|\hat{a}^\dagger\hat{a}|\alpha\rangle = |\alpha|^2$. As a displaced vacuum,

it may be written as $\hat{D}(\alpha)|0\rangle = |\alpha\rangle$, with the well-known displacement operator²

$$\hat{D}(\alpha) = \exp(\alpha\hat{a}^\dagger - \alpha^*\hat{a}). \quad (6)$$

Further, with regard to photon number, the coherent state obeys Poissonian statistics, and can be expanded as

$$|\alpha\rangle = \exp(-|\alpha|^2/2) \sum_{n=0}^{\infty} \frac{\alpha^n}{\sqrt{n!}} |n\rangle. \quad (7)$$

As opposed to the linear displacement operator, the squeezing operator, $\hat{S}(\zeta) = \exp[(\zeta^*\hat{a}^2 - \zeta\hat{a}^{\dagger 2})/2]$, with $\zeta = r \exp(i\phi)$, is quadratic in \hat{a} and \hat{a}^\dagger . Together with the quadratic single-mode phase rotations (by an angle θ),

$$\hat{R}(\theta) = \exp(-i\theta\hat{a}^\dagger\hat{a}), \quad (8)$$

and the quadratic two-mode beam splitter interactions, this completes the linear regime of Gaussian transformations. Note that

$$\hat{R}(\theta)|\alpha\rangle = |\alpha \exp(-i\theta)\rangle, \quad (9)$$

as can be easily understood from Eq. (7).

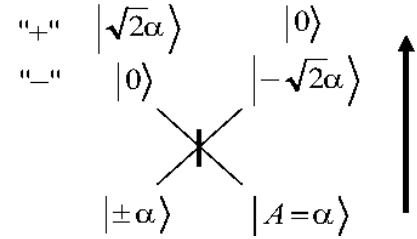


Figure: 2.2.3 Optimal unambiguous state discrimination of equally likely, binary coherent states $\{|\pm\alpha\rangle\}$ using a beam splitter, an ancilla coherent state, and on/off detectors. The inconclusive event here corresponds to the detection of the two-mode vacuum $e^{-\alpha^2}|00\rangle$ for the two output modes with probability $e^{-2\alpha^2}$.

In the linear, CV Gaussian regime, the optical encoding into qumodes (see Fig. 2.2.2) is achieved either through approximate x/p -eigenstates (largely squeezed states), for which projection measurements are well approximated by homodyne detections; alternatively, the overcomplete and nonorthogonal set of coherent states may serve as a basis for qumodes. Perfectly projecting onto this basis is only possible for sufficiently large amplitudes $|\alpha|$, for which the coherent states become near-orthogonal. Nonetheless, two coherent states can also be unambiguously discriminated in the regime of small amplitudes using a beam splitter, an ancilla coherent state, and on/off detectors (see Fig. 2.2.3, α real). This unambiguous state discrimination (USD) is probabilistic, but error-free.

Remarkably, the linear optical scheme for the USD of two arbitrary coherent states [33] such as $\{|\pm\alpha\rangle\}$ achieves

² whenever there is no ambiguity we may drop operator hats.

the quantum mechanically optimal USD for two pure non-orthogonal states $\{|\psi_1\rangle, |\psi_2\rangle\}$, where the success probability for a conclusive result equals $1 - |\langle\psi_1|\psi_2\rangle| = 1 - |\langle\alpha|\alpha\rangle| = 1 - \exp(-2\alpha^2)$ (assuming α real) [34, 35, 36]. For discriminating a larger set of coherent states, optimal USD becomes more subtle. The quantum mechanical optimum for more than two symmetrically distributed coherent states can be approached using linear optics and feedforward [37].

Let us summarize the most common optical resources and potential optical manipulations of qumodes.

Resources: Gaussian states; squeezing by means of $\chi^{(2)}$ nonlinear interactions (optical parametric amplification); non-Gaussian states (e.g., ‘cat states’), producible, in principle, directly from $\chi^{(3)}$ nonlinear interactions.

Processing: Gaussian transformations (LUBOs: phase-space displacements, passive linear optics, active squeezers).

Measurements: Gaussian measurements (e.g., homodyne detection); non-Gaussian measurements (e.g., on/off detectors).

The creation of non-Gaussian resource states such as ‘cat states’ becomes more feasible when conditional state preparation is allowed. In this case, a hybrid approach is useful, as discussed later. A drawback of the CV qumode encoding is that these states are fairly sensitive to losses and noise. The quality of CV Gaussian entangled states, unconditionally and efficiently producible from squeezed light through beam splitters, is fundamentally limited by the constraint of finite squeezing (energy). Fidelities drop quickly in the presence of excess thermal noise, or simply when photons leak into the environment. Nonetheless, most operations are unconditional and homodyne detection is possible with near-unit efficiency.

Finally, once again we note that additional atomic systems and their degrees of freedom may be utilized. In the case of sufficiently large atomic ensembles, the collective spin variables can play the analogous roles of the CV qumode phase-space variables.

2.3. Implementing efficient quantum computation efficiently?

A necessary criterion for a quantum computer to give a true advantage over classical computers is that its realization does not require exponential resources. In other words, the exponential ‘speed-up’ quantum computation is usually associated with must not be at the expense of an exponential increase of physical resources. The exponentially large dimension of the Hilbert space of N logical qubits, 2^N , should be exploited with a number of physical resources scaling as $\sim N$ (or a polynomial of N) rather than $\sim 2^N$. If this criterion is satisfied, the quantum computation is considered to be ‘efficient’.

Besides this theoretical, in-principle ‘efficiency’, an actual physical implementation of a quantum computation

should be experimentally ‘efficient’ as well. While the former type of efficiency is fundamental, the latter one depends on current technology, and an in-principle efficient quantum computation protocol may be infeasible and impractical today, but implementable in the future. Before we shall assess some of the existing proposals for optical quantum computation with regard to these criteria, let us first recall the most commonly used quantum gate sets for DV as well as for CV universal quantum computation.

2.3.1. Universal sets

For several qubits, a combination of arbitrary single-qubit rotations with one fixed two-qubit entangling gate is known to be sufficient for universality such that any unitary gate can be exactly realized on any given multi-qubit state [38]. This universal set, however, is too large (in fact, it is infinitely large) to be implemented in an error-resistant fashion. Therefore, a discrete, finite set of elementary gates must be chosen which no longer achieves exact multi-qubit gates (as the set of unitary gates is continuous), but rather an approximate realization to arbitrary precision. To be efficient, a sufficiently good approximation must not require an exponential number of elementary gate applications. A convenient universal set of gates is

$$\{H, Z_{\pi/2}, Z_{\pi/4}, C_Z\}, \quad (10)$$

where we omitted the operator hats. Here, H is the Hadamard gate, $H|k\rangle = |0\rangle + (-1)^k|1\rangle$, and C_Z acts as an entangling gate, with

$$|k\rangle \otimes |l\rangle \rightarrow (-1)^{kl}|k\rangle \otimes |l\rangle, \quad k, l = 0, 1. \quad (11)$$

The gates $Z_\theta \equiv \exp(-i\theta Z/2)$ describe single-qubit rotations about the Z -axis by an angle θ with Z being one of the usual Pauli operators X, Y, Z , and $Z|k\rangle = (-1)^k|k\rangle$, $X|k\rangle = |k \oplus 1\rangle$. Note that removing the gate $Z_{\pi/4}$ from the elementary gate set means that only so-called Clifford unitaries can be realized which are known to be insufficient for a quantum computational speed-up over classical computation. For both universality and speed-up when computing with computational basis states, the non-Clifford phase gate $Z_{\pi/4}$ must be included here.

Universality for qumodes can be defined and achieved similarly to the qubit case. Arbitrary single-qumode transformations, together with beam splitters for two qumodes, are sufficient to simulate any Hamiltonian expressed as an arbitrary polynomial of the qumode position and momentum operators [8]. As a discrete, elementary gate set for approximate simulations to any precision, one may choose [9]

$$\{F, Z(\tau), D_2(\kappa), D_3(\lambda), C_Z\}, \quad (12)$$

with τ, κ , and λ real.³ In this case, F represents the Fourier transform operator to switch between the position $|\rangle_x$ and

³ commonly, both in the DV and the CV case, the CNOT or SUM gates are used for the canonical entangling gate instead of C_Z ; however, these are equivalent up to local DV-Hadamard or CV-Fourier transformations.

momentum $| \rangle_p$ basis states, $F|x\rangle_x = |x\rangle_p$. The entangling gate C_Z is an x -controlled p -displacement, $C_Z = \exp(2i\hat{x} \otimes \hat{p})$, with

$$C_Z|x\rangle_x|p\rangle_p = |x\rangle_x|p+x\rangle_p, \quad (13)$$

while the roles of the Pauli gates are now played by the Weyl-Heisenberg (WH) momentum and position shift operators, $Z(\tau) = \exp(2i\tau\hat{x})$ and $X(\tau) = \exp(-2i\tau\hat{p})$, respectively, $Z(\tau)|p\rangle_p = |p+\tau\rangle_p$ and $X(\tau)|x\rangle_x = |x+\tau\rangle_x$. Finally, the phase gates $D_l(\kappa_l) = \exp(i\kappa_l\hat{x}^l)$ are included in order to simulate any Gaussian (CV Clifford) transformation ($l = 2$) and to achieve full CV universality including non-Gaussian (CV non-Clifford) gates ($l = 3$). Recall that the Gaussian transformations map Gaussian states onto Gaussian states; they correspond to quadratic Hamiltonians with linear input-output relations for the qumode operators as in Eq. (1). Gaussian operations on Gaussian states can be efficiently simulated classically [9].

Both for the DV and the CV case, for those encodings discussed so far, there is always at least one universal gate that is not realizable through linear transformations alone. In single-photon single-rail encoding, even a single-qubit Hadamard gate, transforming a Gaussian vacuum state into a non-Gaussian superposition of vacuum and one-photon Fock state would be highly nonlinear. The hardest part of universally processing dual-rail encoded qubits would be the entangling gate which has to act upon at least two photons. Ultimately, the universal processing of even a single qumode requires some form of nonlinearity.

2.3.2. Nonlinear versus linear optics

The most obvious approach now to optically implement an entire set of universal quantum gates would be directly through nonlinear interactions. The two-qubit C_Z gate is accomplished by applying a quartic cross-Kerr interaction on two photonic occupation number qubits,

$$\exp(i\pi \hat{a}_1^\dagger \hat{a}_1 \otimes \hat{a}_2^\dagger \hat{a}_2) |k\rangle \otimes |l\rangle = (-1)^{kl} |k\rangle \otimes |l\rangle. \quad (14)$$

The same interaction leads to a C_Z gate for two photonic dual-rail qubits, with the cross-Kerr interaction acting on the second rail (mode) of each qubit such that only the term $|01\rangle \otimes |01\rangle$ acquires a sign flip. This is the conceptually simplest and theoretically most efficient (only one optical device needed!) method to complete the set of universal gates in dual-rail encoding. In the low-photon number subspace here, we may even decompose the cross-Kerr two-mode unitary into a beam splitter, two self-Kerr one-mode unitaries,

$$\exp\left[i\frac{\pi}{2} \hat{a}_1^\dagger \hat{a}_1 (\hat{a}_1^\dagger \hat{a}_1 - 1)\right] \otimes \exp\left[i\frac{\pi}{2} \hat{a}_2^\dagger \hat{a}_2 (\hat{a}_2^\dagger \hat{a}_2 - 1)\right], \quad (15)$$

and another beam splitter (see Fig. 2.3.1).

Thus, a sufficiently strong one-mode self-Kerr interaction would be enough to fulfill the criteria for DV universality [38] on the finite-dimensional multi-qubit subspace of the infinite-dimensional, multi-mode optical Fock

space. At the same time, the quartic one-mode self-Kerr interaction, together with Gaussian, linear transformations (LUBOs), would be also sufficient for the strong notion of full (asymptotically arbitrarily precise) CV universality [8].

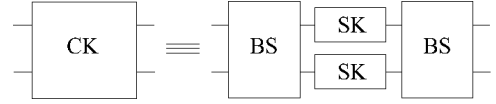


Figure: 2.3.1 Implementing a controlled sign gate (C_Z) on two single-rail qubits using cross-Kerr (CK) or self-Kerr (SK) nonlinearities. The first beam splitter (BS) transforms the term $|11\rangle$ into $|20\rangle - |02\rangle$, while the other terms stay in the vacuum and one-photon space. As the SK interactions affect sign flips only for the two-photon components, only the term $|11\rangle$ acquires a sign flip.

The problem of this approach, however, is that an effective coupling strength of $\sim \pi$ for the self/cross-Kerr interactions is totally infeasible on the level of single photons. Therefore, it is worth examining carefully if there is a way to implement universal quantum gates through linear optical elements, ideally just using beam splitters and phase shifters. A very early proposal for linear-optics-based quantum computation indeed does work with only linear elements [39]. It is based upon so-called multiple-rail encoding, where a d -level system is encoded into a single photon and d optical modes, with the basis states $\hat{a}_k^\dagger |00 \dots 0\rangle$, $k = 1, 2, \dots, d$. Any unitary operator can be realized in the space spanned by this basis, as we only need $\hat{U} \hat{a}_k^\dagger |00 \dots 0\rangle = \sum_{l=1}^d U_{kl} \hat{a}_l^\dagger |00 \dots 0\rangle$, $\forall k$. This linear transformation, as in Eq. (2), is easily achieved through a sequence of beam splitters and phase shifters [29].

As a result, universal quantum computation is, in principle, possible using a single photon and linear optics. This kind of realization would be clearly efficient from an experimental point of view. In fact, implementing a universal two-qubit gate in a $d = 2^2 = 4$ -dimensional Hilbert space, would only require the modest set of resources of an optical ‘ququart’, in ‘quad-rail’ encoding corresponding to a single photon and four optical modes. In fact, for small quantum applications, by adding to the polarization of the photons (their spin angular momenta) extra degrees of freedom such as orbital angular momenta, this kind of approach can be useful [40, 41, 42, 43].

Nonetheless, the drawback of the multiple-rail-based linear-optics quantum computer [39] is its bad scaling. In theory even, this type of quantum computer is inefficient. Scaling it up to computations involving N qubits, we need 2^N basis states, and hence 2^N optical modes. All these modes have to be controlled and processed in a linear optical circuit with an exponentially increasing number of optical elements. For example, a 10-qubit circuit would only require 10 photons and 20 modes in dual-rail encoding, while it consumes $2^{10} = 1024$ modes (for just a single

photon) and at least as many optical elements in multiple-rail encoding.

2.3.3. Teleportation-based approaches

There are now indeed a few proposals that aim at circumventing the in-principle (scaling) inefficiency of the linear multiple-rail protocol and the experimental infeasibility of the direct nonlinear optical approach. Certainly, the two most important and conceptually unique proposals are the KLM [11] and the GKP [10] schemes. In both schemes, a new concept of *measurement-induced nonlinearities* is exploited. The KLM scheme is a fully DV-based protocol, demonstrating that, in principle, passive linear optics and DV photonic auxiliary states are sufficient for (theoretically) efficient, universal DV quantum computation. Inducing nonlinearity through photon counting measurements renders the KLM scheme non-deterministic. However, the probabilistic quantum gates can be made asymptotically near-deterministic by adding to the toolbox feed-forward and complicated, multi-photon entangled auxiliary states with sufficiently high photon numbers, and by employing quantum teleportation [44]. KLM is ‘in-principle efficient’, as the number of the ancillary photons grows only polynomially with the success rate. Fidelities are always, in principle, perfect in the KLM approach.

We shall briefly describe the basic elements of KLM. The GKP scheme combines linear CV resources with linear operations and nonlinear measurements; therefore, a discussion of GKP, which achieves both fault-tolerant DV universality and (non-fault-tolerant) CV universality, in the spirit of Ref. [8], is postponed until the section on hybrid schemes. Similarly, the alternate concept of weak nonlinearities relies on hybrid systems, and will also be discussed later.

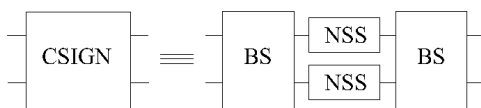


Figure: 2.3.2 Implementing a probabilistic controlled sign gate (CSIGN $\equiv C_Z$) on two single-rail qubits using two non-deterministic NSS gates. The resulting two-qubit gate works in a similar way to the deterministic implementation described in Fig. 2.3.1 using Kerr nonlinearities.

The essential ingredient for the non-deterministic realization of a two-photon two-qubit entangling gate (in dual-rail encoding) is the one-mode nonlinear sign shift (NSS) gate [11]. It acts on the qutrit subspace $\{|0\rangle, |1\rangle, |2\rangle\}$ of the optical Fock space as $|k\rangle \rightarrow (-1)^{k(k-1)/2}|k\rangle$. Placing two such NSS gates in the middle between two beam splitters will then act as a controlled sign gate, $|k\rangle \otimes |l\rangle \rightarrow$

$(-1)^{kl}|k\rangle \otimes |l\rangle$, on two single-rail as well as two dual-rail qubits. In fact, we may replace the deterministic Kerr-based circuit of Fig. 2.3.1 by the equivalent circuit depicted in Fig. 2.3.2. The latter, however, becomes non-deterministic with NSS gates operating only probabilistically.

In the original KLM proposal, the NSS gate can be realized with 1/4 success probability, corresponding to a success probability of 1/16 for the full controlled sign gate as shown in Fig. 2.3.2. In subsequent works, this efficiency was slightly improved [45]. There are also various, more general treatments of these non-deterministic linear-optics gates deriving bounds on their efficiencies [46,47,48]. Experimental demonstrations were reported as well [49], even entirely in an optical fiber [50].

Probabilistic quantum gates cannot be used directly for quantum computation. The essence of KLM (see Fig. 2.3.3) is that near-unit success probabilities are attainable by combining non-deterministic gates on offline entangled states with the concept of quantum gate teleportation [44]. As the necessary Bell measurements for quantum teleportation succeed at most with 1/2 probability, if only fixed arrays of beam splitters are used [51], entangled ancilla states and feedforward must be added to boost efficiencies beyond 1/2 to near 1.

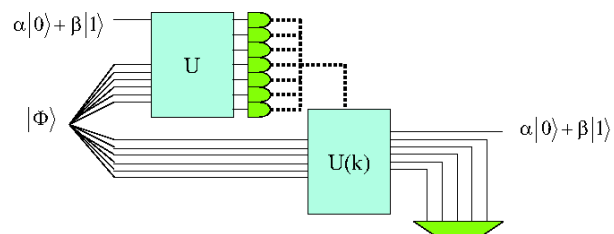


Figure: 2.3.3 Making non-deterministic gates near-deterministic through single-rail quantum teleportation. The Bell measurement is performed by means of the linear-optics circuit U plus photon counting. For an entangled two-mode state $|\Phi\rangle \propto |10\rangle + |01\rangle$ with one ancilla photon, teleportation succeeds only in one half of the cases. For larger ancillae with sufficiently many photons, teleportation can be made almost perfect. In order to teleport a gate near-deterministically onto an input state, the corresponding gate must be first applied offline and probabilistically to the multi-photon entangled ancilla state.

Even though KLM is ‘in-principle efficient’, it is still highly impractical, as near-deterministic operations would require ancilla states too complicated to engineer with current experimental capabilities. It is therefore extremely important to further enhance the efficiencies of linear-optics quantum computation with regard to the resource scaling. Steps into this direction have been made already by merging the teleportation-based KLM approach with the fairly recent concept of one-way (cluster) computation [1].

2.3.4. Cluster-based approaches

In the preceding section, we introduced the notion of measurement-induced nonlinearities, which, combined with the more general (and implementation-independent) concept of measurement-based quantum computation, enables one to obtain the necessary nonlinear element in (linear) optical approaches to quantum information processing. As opposed to the standard, circuit model of quantum computing, where any computation is given by a sequence of reversible, unitary gates, in measurement-based quantum computing, universal quantum gates are encoded ‘offline’ into an entangled-state resource; suitable measurements, performed ‘online’ on this resource state, and, typically, some form of feedforward will then lead to the desired unitary evolution. Feedforward may sometimes be postponed until the very end of the computation, or even totally omitted through ‘reinterpretation’ of the ‘Pauli-frame’; nonetheless, in some form it will be needed in order to render measurement-based quantum computation deterministic despite the randomness induced by the measurements.

There are now further subcategories of measurement-based quantum computing. First, that based on full quantum teleportation [44] involving online *nonlocal* measurements such as Bell measurements, as described in the preceding section. Secondly, there is an ultimate realization of measurement-based quantum computing that requires all entangling operations be done offline and allows only for *local* measurements applied on the offline resource state – the cluster state [1]. In such a cluster computation, a multi-party entangled cluster state is first prepared offline. The actual quantum computation is then performed solely through single-party projection measurements on the individual nodes of the cluster state. By choosing appropriate measurement bases in each step, possibly depending on earlier measurement outcomes, any unitary gate can be applied to an input state which typically becomes part of the cluster at the beginning of the computation, see Fig. 2.3.4.

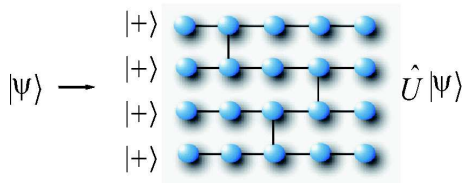


Figure: 2.3.4 One-way (cluster) computation for qubits. Certain single-qubit basis states become pairwise entangled to form a multi-qubit cluster state. Local projection measurements on the individual qubits (potentially including feedforward with a measurement order going from left to right) are then enough to realize universal quantum computation. A multi-qubit input state $|\psi\rangle$ attached to the left end of the cluster could, in principle, be universally processed with the output state occurring at the right end of the cluster. The vertical edges allow for two-qubit gates.

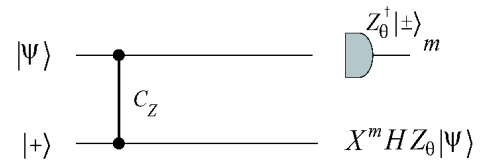


Figure: 2.3.5 Elementary ‘one-bit’ teleportation circuit for qubit cluster computation. The C_Z gate represents a horizontal edge connecting two nodes of the cluster state. An input state $|\psi\rangle$ is teleported into the left node, and a subsequent, local single-qubit measurement in the binary basis $\{Z_\theta^\dagger|\pm\rangle\}$ leaves the second node, up to a Hadamard gate H and a Pauli correction X depending on result $m = 0, 1$, in the unitarily evolved state $Z_\theta|\psi\rangle$, with the rotation angle θ for a Z -rotation $\exp(-i\theta Z/2)$ controlled by the actual choice θ for the measurement basis.

The essence of cluster computation as described by the one-way model of quantum computation [1] can be summarized as follows: the cluster state is *independent of the computation*; universality is achieved through *choice of measurement bases*. This is illustrated in Fig. 2.3.5 for an elementary ‘one-bit’ teleportation circuit between just two nodes of a qubit cluster state; once an input state is part of the cluster (after it got teleported into the cluster), a local single-qubit measurement is then sufficient to apply an arbitrary Z -rotation. At the very beginning of a cluster computation, the cluster computer may be initiated in a product of ‘blank’ basis states $|+\rangle$ such that no extra encoding teleportation step is needed; an arbitrary state can be anyway prepared within the cluster through local measurements. For example, an arbitrary single-qubit rotation requires just three elementary steps as shown in Fig. 2.3.5. In such a concatenation of elementary steps, for a given desired evolution, the later choice of the measurement bases depends on earlier measurement outcomes whenever non-Clifford gates are involved.

Apart from the conceptual innovation, it turned out that, in particular, with regard towards linear optical quantum computation proposals, the cluster approach helps to reduce the resource costs significantly [52,53]. As there are no more nonlocal Bell measurements needed in cluster-based computation, but only local projections, the problem of the nondeterministic linear-optics Bell measurements can be circumvented. Such Bell measurements may only be used for preparing a DV optical cluster state offline [53], whereas the online computation is perfectly deterministic. Eventually, scalability and resource costs in linear-optics quantum computation are determined by the efficiency with which cluster states can be grown using probabilistic entangling gates [54,55].

In a very recent extension of the DV cluster model, the analogous CV cluster computation approach is considered [56]. In the CV model, full CV universality can be approached by applying linear Gaussian and nonlinear non-Gaussian measurements to a Gaussian, approximate CV cluster state. A discussion of universal CV cluster compu-

tation combining CV and DV measurements will be presented in the section on hybrid schemes.

We conclude this section by noting that typically there is a trade-off between the DV and CV optical approaches. The DV schemes are necessarily probabilistic and only at the expense of special extra resources can they be made near-deterministic; fidelities are usually quite high, near-unit fidelities. Conversely, in the CV schemes, fidelities tend to be modest and are necessarily below unity; nonetheless, CV operations are typically deterministic. These characteristic features were already present in the earliest experiments of DV and CV quantum information processing, namely those demonstrating quantum teleportation of an unknown quantum state between two parties [4, 57, 5].

Let us now consider the possibility of optically realizing efficient quantum communication. Even for this supposedly simpler task than universal quantum computation, similar constraints and no-go results exist, when the toolbox is restricted to only linear operations. Especially when efficient and reliable quantum communication is to be extended over large, potentially intercontinental distances, it turns out that this is, in principle, possible, but would require not much less resources than needed for doing optical quantum computation.

2.4. Implementing efficient quantum communication efficiently?

The goal of quantum communication is the reliable transfer of arbitrary quantum states, possibly drawn from a certain alphabet of states. Quantum communication is “the art to transfer quantum states” [58]. This may then lead to various applications such as the secure distribution of a classical key (quantum key distribution [59, 60, 61]) or the connection of spatially separated quantum computers for distributed quantum computing or a kind of quantum internet [62]. As light is an optimal information carrier for communication, one may send quantum states encoded into a stream of single photons or a multi-photon pulse through an optical channel. However, quantum information encoded in fragile superposition states, for example, using photonic qubits or qumodes, is vulnerable against losses and other sources of excess noise along the channel such that the fidelity of the state transfer will exponentially decay with the length of the channel.

For instance, the $|1\rangle = \hat{a}^\dagger|0\rangle$ term of a single-rail qubit would partially leak into the vacuum modes of the channel, $\hat{a}^\dagger|0\rangle \otimes |0\rangle_{\text{ch}} \rightarrow \sqrt{\eta}|10\rangle + \sqrt{1-\eta}|01\rangle$, such that tracing over the channel mode leads to the final signal state $\eta|1\rangle\langle 1| + (1-\eta)|0\rangle\langle 0|$, with the transmission parameter $\eta = \exp(-L/L_{\text{att}})$ and the attenuation length L_{att} . If a photon that did make it through the channel is to be detected and, in particular, resolved against detector dark counts, this will become exponentially harder for longer channels. Similarly, a qumode in a coherent state would be transformed as $|\alpha\rangle \otimes |0\rangle_{\text{ch}} \rightarrow |\sqrt{\eta}\alpha\rangle|\sqrt{1-\eta}\alpha\rangle$, corresponding to the signal map $|\alpha\rangle \rightarrow |\sqrt{\eta}\alpha\rangle$. Although

the coherent state remains pure, its transmitted amplitude would be decreased by an exponential factor. Any non-classical qumode state would exponentially decohere into a mixed state.

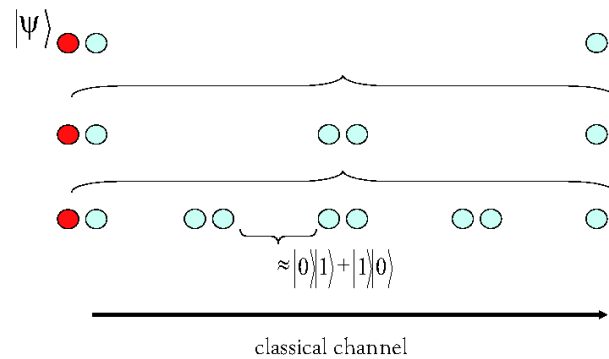


Figure 2.4.1 Concept of a quantum repeater. The state $|\psi\rangle$ is teleported to the remotest station after a long-distance entangled pair is created over the total channel. For this purpose, a supply of short-distance pairs is distributed over sufficiently short channel segments such that high-fidelity entangled pairs can be distilled and connected through entanglement swapping. Only this combination of entanglement distillation and quantum teleportation in a fully nested protocol enables one to suppress the exponential decay of the transfer efficiencies or fidelities as obtained in direct state transmission. As the full protocol typically contains probabilistic elements, sufficient local memories are required.

In long-distance, classical communication networks, signals that are gradually distorted during their propagation in a channel are repeatedly recreated through a chain of intermediate stations along the transmission line. For instance, optical pulses traveling through a glass fiber and being subject to photon loss can be reamplified at each repeater station. Such an amplification is impossible, when the signal carries quantum information. If a quantum bit is encoded into a single photon, its unknown quantum state cannot be copied along the line [63, 64]; the photon must travel the entire distance with an exponentially decreasing probability to reach the end of the channel.

The solution to the problem of long-distance quantum communication is provided by the so-called quantum repeater [2, 3], see Fig. 2.4.1. In this case, prior to the actual quantum-state communication, a supply of standard entangled states is generated and distributed among not too distant nodes of the channel. If sufficiently many of these imperfect entangled states are shared between the repeater stations, a combination of entanglement purification and swapping extends this shared entanglement over the entire channel. Through entanglement swapping [65], the entanglement of neighboring pairs is connected, gradually increasing the distance of the shared entanglement. The entanglement purification [66, 67] enables one to distill (through local operations) a high-fidelity entangled pair

from a larger number of low-fidelity entangled pairs, as they would emerge after a few rounds of entanglement swapping with imperfect entangled states and at the very beginning after the initial, imperfect entanglement generation and distribution between two neighboring repeater stations.

The essence of long-distance quantum communication as realized through the quantum repeater model [2, 3] can be summarized as follows: provided *sufficient local quantum memories* are available and *some form of quantum error detection* is applied, quantum communication over arbitrary distances is possible with an increase of (spatial or temporal) resources scaling only subexponentially with distance. Similar to what we concluded for efficient quantum computation, an in-principle efficient realization depends on a non-exponential resource scaling. Otherwise, without fulfilling this criterion, we could as well choose to directly transmit quantum states, similar to performing exponentially many gate operations in an inefficient quantum computer.⁴

The main distinction between the communication and the computation scenario is that in the former case we may now use probabilistic operations; in particular, quantum error correction may be replaced by quantum error detection. However, this supposed advantage becomes a real advantage only provided that quantum states can be reliably stored during the waiting times for classical signals communicating successful events. So eventually, there is a trade-off between the requirements on memory times and local quantum gates, with the rule of thumb that only less efficient (in terms of fidelity) and more complex quantum error detection/correction schemes would lead to a reduced need for efficient memories [71, 72].

When it comes to turning the in-principle solution to scalable quantum communication over arbitrary distances in form of a quantum repeater into a realistic implementation, what are the currently available resources regarding quantum memories and gates? For a repeater segment of the order of $L_0 \sim L_{\text{att}} \sim 20$ km, with an optical fiber at minimal absorption of 0.17 dB/km corresponding to $L_{\text{att}} \approx 25.5$ km, we have a classical communication time of at least $L_0/c \approx 0.066$ ms (ideally considering the vacuum speed of light c), in order to verify successful entanglement creation, swapping, or distillation events between two neighboring stations. In order to extend this to a total distance of $L \sim 2000$ km, even if no intermediate stations are involved such that only a single heralded entanglement creation event is to be confirmed over the distance L , a classical communication time of about 6.6 ms

⁴ the naive approach of dividing the total channel into several segments that are connected through quantum teleportation without incorporating any form of quantum error detection and without using quantum memories is not enough to render quantum communication efficient with regard to resource scaling; however, it may still help to enhance practicality of a scheme, for instance, in order to resolve single-photon signals against detector dark counts (“quantum relay” [59, 68, 69, 70]).

would be needed. Although memory times approaching 60 ms are achievable in electron spin systems [73], and single excitations may be stored and retrieved over a time scale of 1-10 ms [74, 75], longer memory times would have to rely upon nuclear spins. However, even in this case, currently available memories (~ 1 s [76, 77]) do not match those needed in a fully nested repeater protocol. Moreover, the local quantum logic for error detection (requiring, effectively, a small quantum computer at each station), would further increase the actual memory requirements, for instance, when using probabilistic linear-optics gates [49, 50], as discussed in the preceding section.

The maximum distance for experimental quantum communication is currently about 250 km [78, 59]. Although extensions to slightly larger distances may be possible with present experimental approaches [79], there are also various proposals for actually implementing a quantum repeater. The most recent proposals are based on the non-local generation of atomic (spin) entangled states, conditioned upon the detection of photons distributed between two neighboring repeater stations. The light, before traveling through the communication channel and being detected, is scattered from either individual atoms, for example, in form of solid-state single photon emitters [80, 81], or from an atomic ensemble, i.e., a cloud of atoms in a gas [82] (the ‘DLCZ’ scheme).

In these heralded schemes, typically, the fidelities of the initial entanglement generation are quite high, but the heralding mechanism leads to rather small pair generation rates. Other complications include interferometric phase stabilization over large distances [83, 84, 85, 86] and the purification of atomic ensembles. Yet some elements towards a realization of the DLCZ protocol have been demonstrated already [87, 88, 89, 90].

The DLCZ scheme is initially based upon “hybrid” CV Gaussian entangled states, where hybrid here means that the entanglement is effectively described by a two-mode squeezed state with the two modes being a (symmetric) collective atomic mode for a large ensemble of N_a atoms,

$$\hat{S}_a = \frac{1}{\sqrt{N_a}} \sum_{i=1}^{N_a} |g\rangle_i \langle s|, \quad (16)$$

and a Stokes-light mode, \hat{a}_s [82, 91]; here, $|g\rangle_i, |s\rangle_i$ are the ground and metastable states of the i th atom before and after a Raman transition in a Λ configuration, respectively; $|g\rangle \rightarrow |e\rangle$ is induced by a classical pump (with $|e\rangle$ being the excited state), while $|e\rangle \rightarrow |s\rangle$ produces the forward-scattered Stokes light. In the regime of only low excitations, corresponding to short interaction times t_{int} and Stokes mean photon numbers less than unity, the $n = 0, 1$ terms of the two-mode squeezed state,

$$\frac{1}{\cosh r} \sum_{n=0}^{N_a} (\hat{S}_a^\dagger \hat{a}_s^\dagger \tanh r)^n |0\rangle_a |0\rangle_s / n!, \quad (17)$$

with $|0\rangle_a \equiv \otimes_{i=1}^{N_a} |g\rangle_i$ and “squeezing parameter” r , are dominating such that the resulting atom-light state becomes

approximately $|0\rangle_a|0\rangle_s + r\hat{S}_a^\dagger\hat{a}_s^\dagger|0\rangle_a|0\rangle_s$. To this order, dropping terms $O(r^2)$ and higher, by creating the same state at the nearest repeater station equipped with atomic memories and combining the Stokes fields coming from both stations, labeled by $s1$ and $s2$, at a central beam splitter in order to erase which-path information,

$$\hat{a}_{s1/s2}^\dagger|0\rangle_{s1}|0\rangle_{s2} \rightarrow (\hat{a}_{s1}^\dagger \pm \hat{a}_{s2}^\dagger)|0\rangle_{s1}|0\rangle_{s2}/\sqrt{2}, \quad (18)$$

single-photon detector events would trigger an entangled state of the form $(\hat{S}_{a1}^\dagger \pm \hat{S}_{a2}^\dagger)|0\rangle_{a1}|0\rangle_{a2}/\sqrt{2}$ between the ensembles denoted by $a1$ and $a2$. The initial atom-light entanglement is completely swapped onto the atomic memories. Additional atomic “vacuum” contributions originating from detector dark counts would be (to some extent) automatically removed from the final states; a kind of purification “built into” the entanglement swapping process. The effect of atomic spontaneous emissions is suppressed, because a single atomic spin mode gets collectively enhanced for sufficiently large ensembles $N_a \gg 1$.

Though, in principle, being “fully CV” at the beginning, the DLCZ protocol uses DV measurements with photon detectors in order to conditionally prepare DV entangled states. Ideally only the single excitations from the initial Gaussian states would contribute to the final DV state. Only in this limit (corresponding to small “squeezing” r), we will obtain near-unit fidelity pairs, $F \approx 1 - r^2$, at the expense of longer average creation times, $T \approx T_0/r^2$, with $T_0 \equiv t_{\text{int}} + L_0/c$. In some sense, we could as well add DLCZ to the list of hybrid schemes according to our definition, as it combines (very weakly excited) CV resources with DV measurements, resulting in DV output states.

This is in contrast to the complementary approaches of the Polzik group who use similar physical systems and interactions, i.e., atomic ensembles with Stokes light, but remain fully CV throughout for light-matter teleportations [92] and interfaces [93], as their operations consist of CV homodyne detections and feedforward. In their atom-light CV approach, two orthogonal components of the optical Stokes operators and the atomic collective spin operators are each well approximated by (rescaled) qumode phase-space variables. To sum up, we may say now that in DLCZ effectively “flying qumodes” become “static qubits”, while in Polzik’s schemes, “flying qumodes” become “static qumodes”. The advantage of the latter approach is clearly that it is entirely unconditional with no need for any heralding element; this, as typical in fully CV schemes, is at the expense of only imperfect non-unit fidelities.

In either case, however, the interactions take place in free space, with many atoms effectively enhancing the coupling between the collective spins and the light field. Yet other approaches to quantum communication would turn “flying qubits” (e.g. polarization-encoded photonic qubits) into “static qubits” [59, 80, 81, 94]. Later, in the section on hybrid schemes, we shall describe a scenario in which a single DV spin system (an atomic qubit) is to be entangled with a CV qumode; so then the light-matter coupling is qualitatively different, for instance, taking place and being

enhanced in a cavity, and a “flying qumode” will mediate the entangling interaction between two “static qubits”; as a “genuine” hybrid scheme – the CV qumode component will have to have high excitation numbers as opposed to the single excitations of DLCZ – such a scheme, though not being fully unconditional, will contain an only moderate conditional element.

In summary, all those approaches discussed in this section are still fairly demanding with current technology. Especially, in the DV setting, with its highly conditional entangled-pair creation and connection protocols, the minimal requirements on the necessary quantum memories [95, 96, 97] are far from being met using state-of-the-art resources. Even though a fully CV approach, as implemented in the Polzik experiments, is tempting, because of its unconditionalness for entanglement creation and swapping, entanglement distillation has been shown to be impossible with only Gaussian states and Gaussian operations [98, 99, 100]. So it seems there is always a price to pay when certain types of resources are replaced by supposedly cheaper ones. In the next section, we will now discuss the very recent concept of hybrid quantum information processing, which could be useful for both efficient quantum computation and communication.

3. Hybrid approaches

Let us recall our definition of a hybrid protocol. We refer to a quantum information scheme as hybrid, whenever it is based upon both discrete and continuous degrees of freedom for manipulating and measuring the participating quantum subsystems. In the quantum optical setting, this includes in particular those approaches that utilize light for communication and employ matter systems for storage (and processing) of quantum information [101], as the optical qumodes are most naturally represented by their quantized position and momentum (amplitude and phase quadrature) variables, whereas the atomic spins or any two-level structures in a solid-state system provide the natural realization of qubits. An important ingredient of such hybrid schemes may then be a particularly intriguing form of entanglement – hybrid entanglement, i.e., an inseparable state of two systems of different dimensionality, for example, between a qubit and a qumode.

We shall also remind the reader of the motivation for combining CV and DV approaches, besides the “natural” motivation of representing and using hybrid light-matter systems, as stated in the preceding paragraph. CV Gaussian resources can be unconditionally prepared and Gaussian operations are deterministic and (experimentally) efficient. Nonetheless, there are various, highly advanced tasks which would require a non-Gaussian element:

- quantum error detection and correction for qumodes are impossible in the Gaussian regime [98, 99, 100, 102],
- universal quantum computation on qumodes is impossible in the Gaussian regime [8, 9].

The non-Gaussian element may be provided in form of a DV measurement such as photon counting. There are also a few simpler tasks which can be performed better with some non-Gaussian element compared to a fully Gaussian approach, for instance, quantum teleportation [103] or optimal cloning [104, 105] of coherent states.

Similarly, (efficient) universal quantum computation on photonic qubits would depend on some nonlinear element, either directly implemented through nonlinear optics or induced by photon measurements, as discussed in detail in Sec. 2.3. In addition, there are even supposedly simpler tasks which are impossible using only quadratic interactions (linear transformations) and standard DV measurements such as photon counting. The prime example for this is a complete photonic Bell measurement [12, 13, 14].

It is worth pointing out that the above restrictions and no-go results apply even when linear elements and photon detectors are available that operate with 100% efficiency and reliability (i.e., fidelity). In other words, the imposed constraints are of fundamental nature and cannot be resolved by improving the experimental performance of the linear elements, for example, by further increasing squeezing levels.

Incorporating both nonlinear resources and nonlinear operations into an optical quantum information protocol would enable one, in principle, to circumvent any of the above constraints. Such an approach, unless weak nonlinearities are employed, will most likely be more expensive than schemes that stick to either linear resources or linear operations. There are now many proposals for optically implementing quantum information protocols through a kind of hybrid approach. Among other classifications, two possible categories for such hybrid schemes are:

- those based upon nonlinear resources using linear operations,
- those based on linear resources using nonlinear operations.

In the latter case, for instance, DV photon number measurements may be applied to CV Gaussian resources. The former type of implementations would utilize, for example, CV homodyne measurements and apply them to DV photonic qubit or other non-Gaussian states. Some of these approaches will be presented, with regard to hybrid quantum computing (Sec. 3.3), in Secs. 3.3.3 and 3.3.4, after a discussion on qubit-into-qumode encodings in Sec. 3.3.1 and hybrid Hamiltonians (Sec. 3.3.2). As an additional approach for incorporating a nonlinear element into a quantum information protocol, in Sec. 3.3.5, we shall give a brief description of schemes using weakly nonlinear operations. Finally, we will turn to hybrid quantum communication in Sec. 3.4.

The notion of hybrid entanglement and some of its applications as well as qubit-qumode entanglement transfer will be discussed in Sec. 3.2. As a start, however, let us give a short summary of some earlier hybrid proposals and implementations and some more recent schemes.

3.1. Overview

The hybrid approaches may either aim at “simpler” tasks such as quantum state engineering and characterization, or at the ultimate applications of universal quantum computing and long-distance quantum communication. Here is a short overview on theory and experiments.

Realizing POVMs:

theory: optimal unambiguous state discrimination of binary coherent qumode states $|\pm\alpha\rangle$ using a 50:50 beam splitter, a coherent-state ancilla, and a DV measurement discriminating between zero and nonzero photons (on/off detector) [33] (see Fig. 2.2.3);

theory and experiment: near-minimum error discrimination of $|\pm\alpha\rangle$ using displaced on/off detectors beating the optimal Gaussian homodyne-based discrimination scheme [106].

Quantum state engineering:

generation of Schrödinger-cat (coherent-state superposition, CSS) states with a “size” of $|\alpha|^2 \sim 1.0 - 2.6$; from Gaussian squeezed vacuum through DV photon subtraction using beam splitters and photon detectors, theory [108] and experiment [30, 109, 31, 32]; from squeezed vacuum and one-photon (two-photon) Fock states through beam splitters, CV homodyne detection, and postselection yielding squeezed Fock states and approximate odd (even) CSS states (see Fig. 3.1.1), theory [110] and experiment [111]; experiments: single-mode photon-added/subtracted coherent state [112] and thermal state [113].

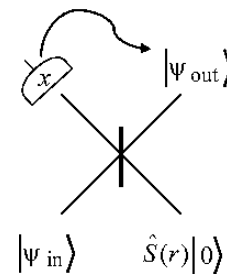


Figure 3.1.1 Conditional preparation of an odd (even) CSS state using DV one-photon (two-photon) Fock states, $|\psi_{in}\rangle = |1\rangle$ ($|\psi_{in}\rangle = |2\rangle$) and CV squeezed vacuum resources, $\hat{S}(r)|0\rangle$, together with CV homodyne detection and postselection [110].

Quantum state characterization:

theory: measurement of entanglement and squeezing of Gaussian states through beam splitters and photon counting [114]; measurement of Bell nonlocality of Gaussian two-mode squeezed states via photon number parity detection [115];

experiment: homodyne tomography of one-photon state [107], homodyne tomography of two-photon state [116].

Quantum communication subroutines:

theory: entanglement concentration (EC) of pure Gaussian two-mode squeezed states (TMSSs) through DV photon

subtraction [117]; entanglement distillation (ED) of noisy Gaussian TMSSs using beam splitters and on/off detectors [118] or photon number QND-measurements [119, 120]; experiment: EC of pure TMSSs through nonlocal [121] and local [122] DV photon subtraction; ED of Gaussian TMSSs subject to non-Gaussian noise such as phase diffusion [123] and random attenuation [124].

Quantum computational resources:

theory: conditional creation of non-Gaussian cubic phase states from TMSSs through DV photon counting, as a resource to implement CV cubic phase gates (GKP, [10]); generalization of such cubic-gate schemes [125]; universal DV gates through weak Kerr-type nonlinearities and strong CV Gaussian probes [126].

More details on the GKP scheme will be presented in Sec. 3.2. The pioneering “hybrid” work is the experiment of Lvovsky *et al.* in which CV, homodyne-based quantum tomography is performed for the discrete one-photon Fock state [107]. The reconstructed Wigner function in this experiment has a strongly non-Gaussian shape including negative values around the origin in phase space.

According to an even earlier, theoretical proposal, CV quantum teleportation [127] is applied to DV entangled states of polarization-encoded photonic qubits [128], transferring DV Bell-type nonlocality through CV homodyne detection and optimized displacements in phase-space for feedforward (“gain tuning”). Optical CV quantum teleportation of DV photonic states was further explored by Ide *et al.* [129, 130], combining CV tools such as gain tuning with postselection, an ingredient inherited from the conditional DV approaches.

It is important to notice that for an experimental implementation of a hybrid scheme in which DV and CV techniques and resources are to be combined (for example, for CV quantum teleportation of DV states), the standard way of applying such methods has to be generalized. In particular, frequency-resolved homodyne detection, as used, for instance, in CV quantum teleportation of coherent states [5], must be extended to time-resolved homodyning [131] in order to synchronize the CV operations with DV photon counting events.⁵ CV operations must act on a faster scale: while the standard CV experiments used single-mode cw light sources with narrow sidebands of ~ 30 kHz, the new generation of hybrid experiments relies upon bandwidths of at least ~ 100 MHz, corresponding to time scales of ~ 100 ns [133].

A beautiful example of a typical hybrid scheme according to our definition is the “offline squeezing” protocol from Ref. [110] for quantum state engineering, experimentally demonstrated in Ref. [111], see Fig. 3.1.1. In

⁵ this extension means that, for instance, measurements on quantum states in the weak-excitation regime are no longer restricted to time-resolved photon counting only (like in the DLCZ repeater proposal), but would include time-resolved homodyning; conversely, an extension from frequency-resolved homodyning to frequency-resolved photon counting could be considered as well [132].

this scheme, approximate CSS states are built using linear CV measurements with outcomes within a finite postselection window, linear CV squeezed-state, and nonlinear DV Fock-state resources. The protocol works by squeezing the input Fock state, e.g., $|1\rangle \rightarrow \hat{S}(r)|1\rangle$, which corresponds approximately to an odd CSS state ($\propto |\alpha\rangle - |-\alpha\rangle$) and would be hard to achieve “online” using the standard squeezing techniques such as optical parametric amplification.⁶ Though postselection renders the protocol probabilistic, it enables one to preserve the non-Gaussianity of the input Fock state. This is different from the non-hybrid “offline squeezing” approach of Refs. [134, 135], where postselection is replaced by a continuous feedforward operation such that “offline squeezing” is applied in a fully Gaussian, deterministic fashion. Later we shall discuss how to realize arbitrary squeezing operations on an arbitrary input state through deterministic, homodyne-based cluster computation.

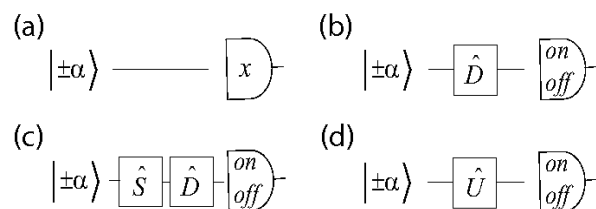


Figure 3.1.2 Approximate discrimination of binary coherent states $\{|\pm\alpha\rangle\}$. Complementary to the probabilistic, error-free USD scheme (Fig. 2.2.3), an appropriate single-mode transformation [(b) optimal displacement \hat{D} , (c) optimal squeezing \hat{S} and displacement \hat{D} , (d) optimal nonlinear non-Gaussian transformation \hat{U}] in front of an on/off photon detector achieves close-to-optimal (b), even closer-to-optimal (c), and optimal (minimum-error) discrimination (d), and would always beat the optimal CV receiver solely based upon homodyne detection (a) [137].

In the non-hybrid, Gaussian CV regime, it is known how useful largely (offline) squeezed states are for engineering all kinds of multi-party entangled states [7] including arbitrary CV graph states [136]. On the other hand, typically, squeezing was explicitly excluded from the toolbox for DV (linear-optical) quantum information processing [6]. One important aspect of the more recent hybrid approaches is that squeezing is no longer considered a resource solely for CV protocols. The above quantum-state-engineering schemes may serve as examples for this.

Besides quantum state engineering, however, there are other tasks in quantum information that may benefit from

⁶ in the experiment of Ref. [111], a two-photon state $|n=2\rangle$ was simply split at a beam splitter; so the squeezed vacuum in Fig. 3.1.1 was just a vacuum state. Postselection through time-resolved homodyne detection led to an output CSS state which was squeezed by 3.5 dB. Theoretically, the fidelity of the CSS state would approach unity for input Fock states $|n\rangle$ with $n \rightarrow \infty$ [111].

the use of squeezing, especially when the squeezing transformation can be applied online to an arbitrary state at any time during a quantum protocol. One example for this is the near-minimum error discrimination of binary coherent-state signals [137], a protocol complementary to the error-free USD as depicted in Fig. 2.2.3. In this case, squeezing is needed to obtain the optimal Gaussian transformation that, in combination with DV photon detection, leads to a near-optimal state discrimination,⁷ see Fig. 3.1.2.

The bottom line of the discussion here is that squeezing added as an online tool to the standard linear-optics toolbox may be of great benefit, beyond the more conventional quantum-state engineering schemes. Further examples are given later in the section on hybrid quantum computing, where squeezing is a necessary correction operation in order to implement nonlinear quantum gates in a measurement-based fashion. Online squeezing could also be used to “unsqueeze” the squeezed CSS state emerging in the experiment of Ref. [111].

Finally, concluding this overview of hybrid proposals and experiments, let us at least mention the ultimate application of CSS states for fault-tolerant, universal quantum computation presented in Ref. [142] and discuss yet another way to create such states [143].

In Section 2.3, we started using the qubit Pauli operator basis X , Y , and Z as elementary gates, and rotations along their respective axes, Z_θ , etc., to describe and realize arbitrary single-qubit unitaries. In analogy, we used a similar notation for the qumode WH (displacement) operator basis, $X(\tau)$ and $Z(\tau)$. Here, in the hybrid context, we shall exploit interactions and operations involving combinations of DV qubit and CV qumode operators and therefore we prefer to use unambiguous notations: for qumodes, still $X(\tau) = \exp(-2i\tau\hat{p})$ and $Z(\tau) = \exp(2i\tau\hat{x})$ for the WH group elements, and \hat{x} and \hat{p} for the Lie group generators with $\hat{a} = \hat{x} + i\hat{p}$; for qubits, now $\sigma_x \equiv X$, $\sigma_y \equiv Y$, and $\sigma_z \equiv Z$ for the Pauli basis. Now look at the effective interaction obtainable from the fundamental Jaynes-Cummings Hamiltonian, $\hbar g(\hat{a}^\dagger\sigma_- + \hat{a}\sigma_+)$, in the dispersive limit [144],

$$\hat{H}_{\text{int}} = \hbar\chi\sigma_z\hat{a}^\dagger\hat{a}. \quad (19)$$

Here, \hat{a} (\hat{a}^\dagger) refers to the annihilation (creation) operator of the electromagnetic field qumode in a cavity and $\sigma_z = |0\rangle\langle 0| - |1\rangle\langle 1|$ is the corresponding Pauli operator for a two-level atom in the cavity (with ground state $|0\rangle$ and excited state $|1\rangle$). The atomic system may as well be an effective two-level system with an auxiliary level (a Λ -system), as described earlier for the DLCZ quantum repeater. However, this time we do not consider the collective spin of many atoms, but rather a single electronic

⁷ The actual optimal (i.e., minimum-error) discrimination would correspond to a projection onto a CSS basis. This so-called Helstrom bound [138] is attainable by replacing the Gaussian transformation in front of the photon detectors by a non-Gaussian one [139], see Fig. 3.1.2. Remarkably, this highly nonlinear, optimal measurement can also be achieved by only photon detection and real-time quantum feedback [140, 141].

spin for a single atom (in a cavity). The operators σ_+ and (σ_-) are the raising (lowering) operators of the qubit. The atom-light coupling strength is determined by the parameter $\chi = g^2/\Delta$, where $2g$ is the vacuum Rabi splitting for the dipole transition and Δ is the detuning between the dipole transition and the cavity field. The Hamiltonian in Eq. (19) generates a controlled phase-rotation of the field mode depending on the state of the atomic qubit. This can be written as ($\theta = \chi t$)

$$\hat{R}(\theta\sigma_z) = \exp(-i\theta\sigma_z\hat{a}^\dagger\hat{a}), \quad (20)$$

which, compared to Eq. (8), now describes a unitary operator that acts in the combined Hilbert space of a single qubit and a single qumode. We may apply this operator upon a qumode in a coherent state, and may formally write

$$\hat{R}(\theta\sigma_z)|\alpha\rangle = |\alpha\exp(-i\theta\sigma_z)\rangle. \quad (21)$$

Compared to the uncontrolled rotation in Eq. (9), this time the qumode acquires a phase rotation depending on the state of the qubit, see Fig. 3.1.3. As the eigenvalues of σ_z are ± 1 , applying $\hat{R}(\theta\sigma_z)$ to the initial qubit-qumode state $|\alpha\rangle \otimes (|0\rangle + |1\rangle)/\sqrt{2}$ results in

$$|\alpha\exp(-i\theta\sigma_z)\rangle \otimes (|0\rangle + |1\rangle)/\sqrt{2} \\ = (|\alpha e^{-i\theta}\rangle|0\rangle + |\alpha e^{i\theta}\rangle|1\rangle)/\sqrt{2}, \quad (22)$$

a hybrid entangled state between the qubit and the qumode.

The observation that this hybrid entangled state can be used for creating a macroscopic superposition state of a qumode, a CSS state, by measuring the microscopic system, the qubit, is about 20 years old [143]. A suitable measurement is a projection onto the conjugate σ_x qubit basis, $\{|\pm\rangle\}$, equivalent to a Hadamard gate applied to the qubit,

$$(|\alpha e^{-i\theta}\rangle|+\rangle + |\alpha e^{i\theta}\rangle|-\rangle)/\sqrt{2}, \quad (23)$$

followed by a qubit computational σ_z measurement. Depending on the result, we obtain $\propto |\alpha e^{-i\theta}\rangle \pm |\alpha e^{i\theta}\rangle$ for the qumode. The size of this CSS state depends on the distance between the rotated states in phase space, see Fig. 3.1.3, scaling as $\sim \alpha\theta$ for typically small θ values. However, sufficiently large initial amplitudes α still lead to arbitrarily “large” CSS states (at the same time increasing their vulnerability against photon losses).

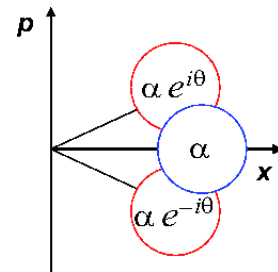


Figure: 3.1.3 Controlled phase rotation of a qumode in a coherent state, α real. Depending on the qubit state, $\sigma_z = \pm 1$, the phase angle of the controlled rotation will be $\mp\theta$. When the qubit starts in a superposition state, $\propto |0\rangle + |1\rangle$, we obtain a hybrid entangled state between the qubit and the qumode.

This is a manifestation of a weak nonlinearity which is effectively enhanced through a sufficiently intense light field. Although typically the “single-atom dispersion” itself is rather weak with small phase angles of at most $\theta \sim 10^{-2}$, it does not require strong coupling; in a CQED setting, the only requirement is a sufficiently large cooperativity parameter [145]. In the following sections, we shall also consider using weak nonlinearities for certain quantum gate constructions and, more generally, sets of hybrid operations such as controlled displacements and rotations sufficient for universal quantum computing.

Essential part of any such protocol is the generation of hybrid entanglement, as expressed by Eq. (22). Then measuring the qubit appropriately yields macroscopic CSS states, as described; measurements on the qumode may be useful for creating entangled qubit memory pairs in quantum communication, and, for the ultimate application, no measurements at all may still give universal quantum gates, as shown later. Let us now look in a little more detail at the notion of hybrid entanglement.

3.2. Hybrid entanglement

In the preceding section, we encountered the example of an entangled state between a qubit and a qumode. This state, though defined in a combined qubit-qumode, hence infinite-dimensional Hilbert space, can be formally written in a two-qubit Hilbert space, as we shall explain in this section. Thus, the entanglement of this state can be conveniently quantified.

Besides entanglement measures for quantifying entanglement, entanglement qualifiers, so-called entanglement witnesses, have become useful tools for delineating inseparable states. Such witnesses are well-known for CV Gaussian states [146, 147] as well as for DV density operators [148]. Optically encoded quantum information, however, may comprise DV photonic qubit states in a Fock subspace or general non-Gaussian entangled states. Using the partial transposition inseparability criteria [149, 148], Shchukin and Vogel demonstrated that certain inseparability criteria for states living in a physical bipartite space of two qumodes can be unified under one umbrella in terms of a hierarchy of conditions for all moments of the mode operators [150] (their results were further refined by Miranowicz and Piani [151]). These general conditions then include the previously known criteria expressed in terms of second moments [146, 147] as a special case, even those believed to be independent of partial transposition [146]. For non-Gaussian entangled states, the second-moment criteria would typically fail to detect entanglement, and a possible entanglement witness would have to incorporate higher-order moments.

Another interesting aspect when comparing qubit and qumode entangled states is whether the readily available, naturally given amounts of potentially unbounded CV entanglement can be transferred onto DV qubit systems [152, 153]. In the following subsection, we shall first consider

qubit-qumode hybrid entangled states, including a discussion on how to witness and possibly quantify their entanglement. Further, we will devote another subsection to the topic of transferring entanglement between qubit and qumode systems.

3.2.1. Qubit-qumode entangled states

Consider the following bipartite state,

$$(|\psi_0\rangle|0\rangle + |\psi_1\rangle|1\rangle) / \sqrt{2}, \quad (24)$$

with an orthogonal qubit basis $\{|0\rangle, |1\rangle\}$ and a pair of linearly independent qumode states $|\psi_0\rangle$ and $|\psi_1\rangle$. A specific example of such a state and a possible way to build it was presented in Eq. (22) and the preceding discussion.

Clearly, the state in Eq. (24) becomes a maximally entangled, effective two-qubit Bell state when $\langle\psi_0|\psi_1\rangle \rightarrow 0$. For $0 < |\langle\psi_0|\psi_1\rangle| < 1$, the state is nonmaximally entangled, but still can be expressed effectively as a two-qubit state. This can be seen by writing the two pure, nonorthogonal qumode states in an orthogonal, two-dimensional basis, $\{|u\rangle, |v\rangle\}$,

$$\begin{aligned} |\psi_0\rangle &= \mu|u\rangle + \nu|v\rangle, \\ |\psi_1\rangle &= (\mu|u\rangle - \nu|v\rangle) e^{i\phi}, \end{aligned} \quad (25)$$

where $\nu = \sqrt{1 - \mu^2}$ with $\mu = [1 + e^{-i\phi}\langle\psi_0|\psi_1\rangle]^{1/2} / \sqrt{2}$. Then, using this orthogonal basis,

$$\begin{aligned} |u\rangle &= (|\psi_0\rangle + e^{-i\phi}|\psi_1\rangle) / (2\mu), \\ |v\rangle &= (|\psi_0\rangle - e^{-i\phi}|\psi_1\rangle) / (2\nu), \end{aligned} \quad (26)$$

the hybrid entangled state of Eq. (24) becomes

$$\mu|u\rangle|0\rangle + \sqrt{1 - \mu^2}|v\rangle|1\rangle, \quad (27)$$

a nonmaximally entangled two-qubit state with Schmidt coefficients μ and $\sqrt{1 - \mu^2}$, where 1 ebit is obtained only for $\mu \rightarrow 1/\sqrt{2}$ and $\langle\psi_0|\psi_1\rangle \rightarrow 0$. Quantifying the entanglement is straightforward, as the entropy of the reduced density matrix is a function of the Schmidt coefficients.

It is interesting to compare the state of Eq. (24) with a bipartite qumode-qumode entangled state of the form

$$(|\psi_0\rangle|\psi_0\rangle \pm |\psi_1\rangle|\psi_1\rangle) / \sqrt{N_{\pm}}, \quad (28)$$

assuming the overlap $\langle\psi_0|\psi_1\rangle$ is real [154]. First of all, in this case, a normalization constant N_{\pm} is needed, depending on $\langle\psi_0|\psi_1\rangle$. Secondly, and quite remarkably, such a state may always represent a maximally entangled two-qubit state (in the subspaces spanned by $|\psi_0\rangle$ and $|\psi_1\rangle$), independent of $\langle\psi_0|\psi_1\rangle$, but depending on the relative phase [154, 155, 156], i.e., the sign in Eq. (28).

The prime example for such qumode-qumode entangled states are two of the so-called quasi-Bell states,

$$|\Psi^{\pm}\rangle \equiv (|\alpha\rangle|\alpha\rangle \pm |-\alpha\rangle|-\alpha\rangle) / \sqrt{N_{\pm}}, \quad (29)$$

with $N_{\pm} \equiv 2 \pm 2e^{-4|\alpha|^2}$. The state $|\Psi^{-}\rangle$ is identical to the two-qubit Bell state $(|u\rangle|v\rangle + |v\rangle|u\rangle) / \sqrt{2}$ when $2\mu =$

$\sqrt{2 + 2e^{-2|\alpha|^2}}$, $2\nu = \sqrt{2 - 2e^{-2|\alpha|^2}}$, and $N_- = 8\mu^2\nu^2$, which is maximally entangled with exactly 1 ebit of entanglement for *any* $\alpha \neq 0$. In contrast, the state $|\Psi^+\rangle$ only equals the one-ebit Bell state $(|u\rangle|u\rangle + |v\rangle|v\rangle)/\sqrt{2}$ in the limit of orthogonal coherent states, $\langle\alpha|-\alpha\rangle \rightarrow 0$ for $\alpha \rightarrow \infty$.⁸

The amount of entanglement in the qubit-qumode and qumode-qumode states of Eqs. (24) and (28), respectively, is bounded above by one ebit, corresponding to a maximally entangled two-qubit Bell state. This is different from a “genuine” CV qumode-qumode entangled state such as a Gaussian two-mode squeezed state, which contains an arbitrary amount of entanglement for sufficiently high levels of squeezing, see Fig. 3.2.1 in the next section.⁹

Let us further mention that the quantification of entanglement of the hybrid states in Eqs. (24) and (28) (we may also refer to the latter as hybrid in the sense that the two physical qumodes each effectively live in a two-dimensional logical subspace) becomes more subtle, when they are mapped onto mixed states. For example, a qumode could be subject to an imperfect channel transmission, for instance, in a lossy fiber. Then for the special case of $|\psi_0\rangle$ and $|\psi_1\rangle$ being coherent states do we still obtain qubit-like expressions, as the coherent states themselves remain pure under amplitude damping (and the resulting mixed states would be expressible and hence quantifiable as two-qubit density operators in the orthogonal $\{|u\rangle, |v\rangle\}$ -basis, see, for example, Ref. [160]). In this case, the density operator decoheres faster for larger amplitudes α ; an effect which will become important later in the hybrid quantum communication schemes.

Finally, it is worth pointing out that lower bounds on the entanglement of (pure or mixed) non-Gaussian entangled states such as those pure-state examples in Eq. (29) can be derived from the standard measures for Gaussian entanglement [161,162] by simply calculating the entanglement for the Gaussian state with the same second-moment correlation matrix as the non-Gaussian state given; in other words, *for a given correlation matrix, the corresponding Gaussian-state entanglement provides a conservative and hence safe estimate on the actual entanglement of the state in question* [163].¹⁰

Apart from applying entanglement measures to hybrid and non-Gaussian entangled states, it is sometimes enough to have a (theoretical and, in particular, experimental) tool

⁸ similarly, for the other two (quasi-)Bell states, we then have $|\alpha\rangle|-\alpha\rangle - |-\alpha\rangle|\alpha\rangle \propto |u\rangle|v\rangle - |v\rangle|u\rangle$ for *any* value of α , but $|\alpha\rangle|-\alpha\rangle + |-\alpha\rangle|\alpha\rangle \propto |u\rangle|u\rangle - |v\rangle|v\rangle$ only when $\alpha \rightarrow \infty$.

⁹ the entropy of the reduced density matrix of a two-mode squeezed state, i.e., its entanglement would exceed one ebit at about 4.5 dB squeezing. Thus, the currently available squeezing levels of about 10 dB [157,158,159], corresponding to about 3 ebits (see Fig. 3.2.1), would easily suffice to outperform those hybrid entangled states discussed in the present section.

¹⁰ note that Gaussian states also provide an upper bound on the entanglement when only the correlation matrix is known: for given energy, Gaussian states maximize the entanglement [164].

in order to decide whether a given state is entangled or not. Such entanglement qualifying criteria are typically related with certain observables (Hermitian operators) \hat{W} for which the expectation value $\text{Tr}(\rho\hat{W})$ is nonnegative for all separable states ρ , whereas it may take on negative values for some inseparable states ρ . Entanglement witnesses are well-known for CV Gaussian states [146,147] as well as for DV density operators [148].

Qumode-qumode entangled states like those in Eq. (28) may be identified through the partial transposition criteria [149,148] adapted to the case of arbitrary CV states [150,151]. As a result, all known CV inseparability criteria, including those especially intended for Gaussian states and expressed in terms of second moments [146,147], can be derived from a hierarchy of conditions for all moments of the mode operators \hat{a} and \hat{a}^\dagger . Moreover, for non-Gaussian entangled states, for which the second-moment criteria typically fail to detect entanglement, the higher-moment conditions would work. The concept for these criteria is as follows.

It is known that for any positive operator $\hat{P} \geq 0$, we can write $\hat{P} = \hat{f}^\dagger \hat{f}$ such that $\text{Tr}(\rho \hat{f}^\dagger \hat{f})$ is nonnegative for any operator \hat{f} and any physical state ρ . Then we may choose the bipartite decomposition $\hat{f} = \sum_{ij} c_{ij} \hat{A}_i \otimes \hat{B}_j$, for which

$$\begin{aligned} 0 &\leq \text{Tr}(\rho \hat{f}^\dagger \hat{f}) \\ &= \sum_{ij,kl} c_{ij}^* \text{Tr}(\rho \hat{A}_i^\dagger \hat{A}_k \otimes \hat{B}_j^\dagger \hat{B}_l) c_{kl} \\ &\equiv \sum_{ij,kl} c_{ij}^* [M(\rho)]_{ij,kl} c_{kl}, \end{aligned} \quad (30)$$

for any coefficients c_{ij} . Hence the matrix $M(\rho)$ is positive-semidefinite for any physical state ρ . Now any separable state ρ remains a physical state after partial transposition of either subsystem such that $M(\rho^{T_A})$ and $M(\rho^{T_B})$ remain positive-semidefinite matrices, where T_A and T_B denotes partial transposition for subsystem A and B , respectively. Then, negativity of $M(\rho^{T_A})$ or $M(\rho^{T_B})$, and hence negativity of any subdeterminant of $M(\rho^{T_A})$ or $M(\rho^{T_B})$ is a sufficient criterion for entanglement, from which sets of inequalities can be derived with convenient choices for the local operators \hat{A}_i and \hat{B}_j [150].

One such choice for a qumode-qumode state would be each qumode’s position and momentum operators, eventually reproducing Simon’s criteria in terms of second-moment correlation matrices [147]. Another choice, adapted to a qubit-qumode state of the form in Eq. (24), is given by $\{\hat{A}_i\} = \{|\phi\rangle\langle 0|, |\phi\rangle\langle 1|\}$ and $\{\hat{B}_j\} = \{\mathbb{1}, \hat{x}, \hat{p}\}$, with some generic qubit state $|\phi\rangle$ [165]. The resulting expectation value matrix $M(\rho)$ then serves again, using partial transposition, as a tool to detect entanglement, this time for hybrid qubit-qumode states. This can be particularly useful for verifying the presence of effective entanglement in a binary coherent-state-based quantum key distribution protocol [166,167] as a necessary security requirement [168].

The choices for the local operators \hat{A}_i and \hat{B}_j discussed so far all lead to second-moment conditions only. These are experimentally most accessible, but may fail to detect some form of non-Gaussian entanglement. For qumode-qumode states, a more general choice is the normally ordered form for \hat{f} , $\hat{f} = \sum_{nmkl} c_{nmkl} \hat{a}^{\dagger n} \hat{a}^m \hat{b}^{\dagger k} \hat{b}^l$, with mode operators \hat{a} and \hat{b} for the two qumodes A and B , respectively. Inserting this into $\text{Tr}(\rho^{T_A} \hat{f}^\dagger \hat{f}) \geq 0$ or $\text{Tr}(\rho^{T_B} \hat{f}^\dagger \hat{f}) \geq 0$ yields a hierarchy of separability conditions in terms of the moments of the mode operators. For example, the quasi-Bell state $|\Psi^-\rangle$ of Eq. (29) leads to a subdeterminant of the matrix of moments with a sufficient order of the moments such as $\langle \hat{a}^\dagger \hat{a} \hat{b}^\dagger \hat{b} \rangle$ which becomes $-\alpha^6 \frac{\coth(2\alpha^2)}{\sinh^2(2\alpha^2)} \equiv s$, for real α [150, 151]. This subdeterminant is negative for any nonzero α , proving the entanglement of the state $|\Psi^-\rangle$ for any $\alpha \neq 0$.¹¹

To conclude this section, let us summarize that it is straightforward to quantify the entanglement of hybrid qubit-qumode and non-Gaussian qumode-qumode states, provided these states can be represented in two-dimensional subspaces. Otherwise, in order to detect the inseparability of such states, the partial transposition criteria expressed in terms of matrices of moments can be used. In a recent experiment, employing CV quantum information encoded into the spatial wavefunction of single photons, fourth-order-moment entanglement was detected [169].

3.2.2. Qubit-qumode entanglement transfer

As the entanglement in Gaussian qumode states is unconditionally available and, in principle, unbounded, it is tempting to consider protocols in which the CV entanglement is transferred onto DV systems. Especially the local memory nodes in a quantum repeater are typically represented by atomic spin states (recall the discussion in Sec. 2.4). So the unconditional generation of CV entanglement and its efficient distribution between two repeater stations should then be supplemented by a transfer of the transmitted ebits (in form of flying qumodes) onto the local, electronic or nuclear, storage spins (in form of static qubits).

Consider the distribution of two-mode squeezed states, $\sum_{n=0}^{\infty} \tanh^n r |n, n\rangle / \cosh r$, with squeezing r . In principle, an amount of entanglement in ebits [170],

$$E(r) = \cosh^2 r \log_2(\cosh^2 r) - \sinh^2 r \log_2(\sinh^2 r), \quad (31)$$

could then be shared between the ends of the channel. Realistically, of course, the entanglement distribution will be subject to photon losses, leading to a highly degraded, shared CV entanglement; though always a nonzero amount of entanglement remains, unless additional thermal noise sources are present along the channel [146]. We shall take

¹¹ note that $s \rightarrow 0$ for $\alpha \rightarrow \pm\infty$ and that s is maximally negative, $s \approx -0.125$, for $|\alpha| < 0.4$, even though we know that $|\Psi^-\rangle$ has constant entanglement of one ebit for any nonzero α .

into account lossy channels in a later section. In this section, let us neglect the imperfect channel transmission and consider ideal CV entanglement distribution. In this case, Fig. 3.2.1 shows how many ebits could be, in principle, transferred from the CV to the DV system. Figure 3.2.2 illustrates the principle of entanglement distribution and transfer.

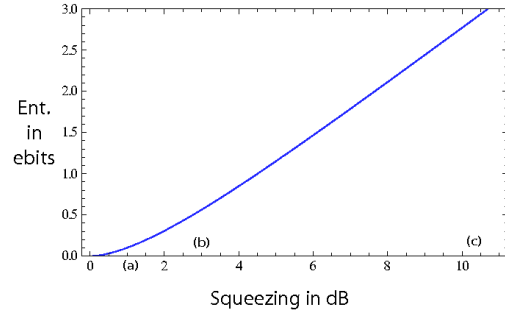


Figure 3.2.1 Entanglement of a Gaussian two-qumode squeezed state in ebits (the units of maximally entangled two-qubit states) as a function of the squeezing values in dB. The letters indicate experiments with corresponding squeezing levels: (a) recent CV Shor-type quantum error correction scheme [171], (b) first CV quantum teleportation [5], and (c) most recent squeezing “world records” [157, 158, 159].

So what mechanism achieves this entanglement transfer? Are there possibly fundamental complications owing to the mismatch of the Hilbert spaces?¹² These questions were addressed in Refs. [172, 173, 174], where it was shown that an entangled two-mode squeezed state may act as a driving field to two remote cavities. When a two-level system is placed in each cavity, the resonant Jaynes-Cummings Hamiltonian, $\hbar g(\hat{a}^\dagger \sigma_-^a + \hat{a} \sigma_+^a)$, can be used, describing the qubit-qumode coupling for qumode \hat{a} and qubit σ_-^a , and similarly for mode \hat{b} and spin σ_-^b . As the driving field is assumed to be an external, broadband field, an additional interaction has to be included that describes the desired coupling between the external qumodes $\hat{a}_k e^{i\omega_k t}$ and the internal cavity qumode \hat{a} (and similar for the internal and external qumodes \hat{b} and $\hat{b}_k e^{i\omega_k t}$, respectively), $\sum_k \kappa_k [\hat{a} \hat{a}_k^\dagger e^{i(\omega_a - \omega_k)t} + \hat{a}^\dagger \hat{a}_k e^{-i(\omega_a - \omega_k)t} + a \leftrightarrow b]$ [174]. Thus, κ_k is the rate of this wanted coupling between each internal qumode at frequency $\omega_{a,b}$ and a corresponding external driving qumode at frequency ω_k . In the weak-coupling regime, where κ is much smaller than the external bandwidth, the non-unitary dynamics of the (internal) qumode-qubit systems is governed by a master equation. The steady state of the cavities can then be shown to become a two-mode squeezed state (in the bad-cavity regime using CQED language [175]).

¹² later, for a hybrid quantum repeater, we can avoid this mismatch from the beginning by distributing effective two-qubit entanglement of the form of hybrid qubit-qumode states.

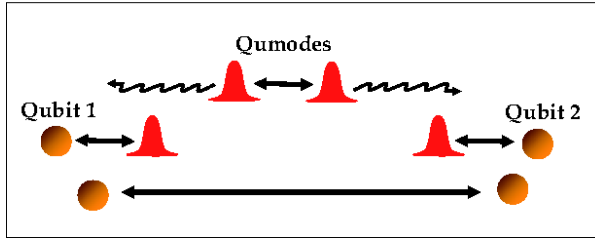


Figure 3.2.2 Using a CV entanglement distributor for DV entanglement distribution. Two entangled qumode pulses travel to the opposite ends of a channel and interact with local atomic qubits placed, for instance, in a cavity. Through these interactions, the CV entanglement is dynamically transferred onto the two qubits.

Eventually, the CV entanglement is transferred onto the DV systems in the steady state. More realistically, additional dissipations have to be taken into account such as spontaneous atomic decay. This kind of unwanted in-out coupling will occur at a rate Γ . An important parameter then is the so-called cooperativity, $C \propto 1/(\Gamma\kappa)$. Only for sufficiently large C do we obtain a nearly pure atomic steady state [174].¹³

The general conditions for transferring general CV entanglement (including non-Gaussian entanglement of the form Eq. (29)) from CV driving fields onto two qubits, both for the dynamical and the steady-state cases, were presented in Ref. [174]. Similar DV entanglement generation schemes were proposed in Refs. [176] and [177] using an indirect interaction of two remote qubits through Markovian and non-Markovian environments, respectively. Finally, let us mention the interesting concept of transferring entanglement from a relativistic quantum field in a vacuum state onto a pair of initially unentangled atoms [178, 179].

Different from those schemes described in this section, which are basically measurement-free and dynamical entanglement transfer protocols utilizing an optical field as entanglement distributor, later we shall describe how to exploit local measurements on hybrid entangled states in order to nonlocally prepare entangled qubit states. The optical field will then act as a kind of quantum bus mediating the interaction between the qubits.

3.3. Hybrid quantum computing

In this section, we shall now discuss various hybrid approaches to quantum computing. This includes optical hybrid protocols for models of universal quantum computation as well as for certain gates from a universal gate set.

¹³ however, the assumption of large C may collide with the bad-cavity/weak-coupling assumption [174, 175]. Later, in the section on hybrid quantum communication, the hybrid quantum repeater shall also depend on sufficiently large C [145].

More specifically, for processing photonic quantum information, we consider either using linear optical resources such as Gaussian entangled cluster states and performing nonlinear operations on them, or first creating offline nonlinear, non-Gaussian resource states and applying linear operations such as homodyne detections. Further, we discuss hybrid schemes for quantum computing and universal quantum logic that do not require any highly nonlinear resources or interactions: only a weakly nonlinear element is needed [17].

However, let us start this section by looking at a few proposals in which either the encoding of quantum information [10, 142] or the unitary gate evolutions, i.e., the interaction Hamiltonians [180], are explicitly hybrid.

3.3.1. Encoding qubits into qumodes

There are various ways to encode a photonic qubit into optical modes such as polarization or spatial modes, as we discussed in the introductory part of this article. In particular, the photon occupation number in a single-rail, single-mode Fock state may serve as a qubit or a more general DV basis. In dual-rail or, more generally, multiple-rail encoding, a single photon encoded into multi-mode states can be even universally processed through linear optical elements; though in an unscalable fashion, unless complicated ancilla states and feedforward are employed [11].

Another natural way to encode a logical DV state into a physical, optical multi-mode state would be based upon at least two qumodes and a constant number of photons distributed over the physical qumodes such that, for example, a logical, $2J + 1$ -dimensional spin- J state, $|J, m_j\rangle$, $m_j = -J, -J + 1, \dots, J - 1, J$, can be represented by two physical qumodes in the two-mode Fock state $|J \equiv (n_1 + n_2)/2, m_j \equiv (n_1 - n_2)/2\rangle$, where n_1 and n_2 denote the photon numbers of the two modes.¹⁴ In fact, for $n_1 + n_2 = 1$, we obtain a dual-rail encoded spin-1/2 qubit: $\{|J = 1/2, m_j = -1/2\rangle, |J = 1/2, m_j = +1/2\rangle\} \equiv \{|n_1 = 0, n_2 = 1\rangle, |n_1 = 1, n_2 = 0\rangle\}$. Similarly, a spin-1 qutrit, $\{|J = 1, m_j = -1\rangle, |J = 1, m_j = 0\rangle, |J = 1, m_j = 1\rangle\}$ corresponds to $\{|0, 2\rangle, |1, 1\rangle, |2, 0\rangle\}$ in the Fock basis.

These natural encodings may even automatically provide some resilience against certain errors such as photon losses. For instance, the dual-rail encoding serves as an error detection code [11, 38], and multi-photon states

¹⁴ the choice of constant total number $\hat{n}_1 + \hat{n}_2 \equiv \hat{S}_0$ and varying number differences $\hat{n}_1 - \hat{n}_2 \equiv \hat{S}_3$ corresponds to a specific basis in the so-called Schwinger representation. For example, in order to faithfully represent the SU(2) algebra by the Lie algebras of two infinite-dimensional oscillators, i.e., two qumodes \hat{a}_1 and \hat{a}_2 , one may replace the usual Pauli matrices $\sigma_0 \equiv \mathbf{1}$, $\sigma_1 \equiv \sigma_x$, $\sigma_2 \equiv \sigma_y$, and $\sigma_3 \equiv \sigma_z$ by the so-called quantum Stokes operators $\hat{S}_i = (\hat{a}_1^\dagger, \hat{a}_2^\dagger)\sigma_i(\hat{a}_1, \hat{a}_2)^T$, $i = 0, 1, 2, 3$, satisfying the SU(2) Lie algebra commutators $[\hat{S}_1, \hat{S}_2] = 2i\hat{S}_3$, while $[\hat{S}_0, \hat{S}_j] = 0$, for $j = 1, 2, 3$.

subject to losses may also keep high degrees of entanglement [182]. However, for the purpose of fault-tolerant, universal quantum information processing, other encodings could be preferable, though they might be much harder to realize. One example is the fault-tolerant quantum computation proposal based upon CSS states such as the qubit-type states $(a|\alpha\rangle + b|-\alpha\rangle)/\sqrt{N}$, $N = |a|^2 + |b|^2 + 2e^{-2|\alpha|^2}\text{Re}(ab^*)$ [142]. Although some universal DV gates such as the Hadamard gate (possibly using auxiliary hybrid entangled states of the form in Eq. (29) for a teleportation-based realization) are hard to implement for this encoding, the effect of photon losses on these CSS-type states corresponds to random phase flips in the coherent-state basis such that repetition codes known from DV qubit quantum error correction can be directly applied [181]. Nonetheless, these codes would still require Hadamard gates for encoding and decoding.

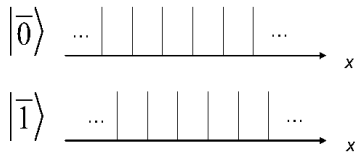


Figure 3.3.1 Encoding a qubit into a qumode according to GKP [10]. The logical, computational qubit basis states, with $\bar{Z}|k\rangle = (-1)^k|\bar{k}\rangle$, $k = 0, 1$, are infinite superpositions of delta peaks in position space. This encoding is particularly suited to protect the qubit against small, diffusive shift errors as arising from, for instance, weak amplitude damping of the qumode.

Another well-known proposal for fault-tolerant, universal quantum computation on logical qubits encoded into a physical qumode space is the GKP scheme [10]. This type of encoding (see Fig. 3.3.1) is primarily intended to protect a logical qubit against small errors such as small shifts of the physical qumode in phase space. Direct translations of standard qubit quantum error correction codes against rarely occurring Pauli errors into the CV regime [183, 184, 185] fail to provide any protection against such small, diffusive, typically Gaussian errors [102]. Provided the error shifts are sufficiently small, i.e., smaller than $\Delta/4$ with Δ the distance between the delta peaks in Fig. 3.3.1, the encoded states remain sufficiently intact, and suitable syndrome measurements enable one, in principle, to detect the errors and correct the states.

Besides having this special error correction capability, the GKP scheme also includes universal gate operations. The link between logical and physical gate operations can be easily understood from Fig. 3.3.1.¹⁵ A logical Pauli op-

¹⁵ in Fig. 3.3.1, we do not show the logical eigenstates of the logical \bar{X} Pauli operator. Similar to the logical eigenstates of the

erator $U \in \{\bar{X}, \bar{Y}, \bar{Z}\}$ is transformed under conjugation by a logical qubit Clifford unitary C into a different logical Pauli operator, $C^\dagger U C = U' \in \{\bar{X}, \bar{Y}, \bar{Z}\}$. Thus, as the logical Pauli gates correspond to WH shifts of the physical qumode, any physical Gaussian operation, since it preserves such WH gates under conjugation, can only lead to a logical Clifford operation. Therefore, *a physical non-Gaussian operation is needed in order to achieve logical non-Clifford qubit gates and hence DV qubit universality*. GKP demonstrate two such non-Clifford gates of which one uses a controlled rotation through a dispersive atom-light interaction as in Eq. (20), whereas the other one is based upon a cubic phase gate on the physical qumode, $D_3(\kappa_3) = \exp(i\kappa_3\hat{x}^3)$. Recall that this gate can also be used to complete the universal set for full CV universality in Eq. (12), in the spirit of Ref. [8].

In optical quantum information processing, it is pretty natural to encode DV quantum information into an appropriate subspace of the full infinite-dimensional qumode space. However, in order to realize the most advanced optical quantum processors, which achieve both universality and fault tolerance, the qubit-into-qumode encodings, though conceptually highly interesting, may still be far from being implementable. In this sense, the CSS-type encoding [142] and the position/momentum-eigenstate superposition encoding à la GKP [10] are very similar. In both schemes, fault tolerance and universality require complicated non-Gaussian operations or resources. Nonetheless, they do both incorporate the necessary non-Gaussian quantum error correction steps into a DV qubit processor embedded in the physical space of an optical qumode.

3.3.2. Hybrid Hamiltonians

Besides the qubit-into-qumode encodings of the preceding section, another interesting hybrid approach is based upon unitary evolutions, i.e., Hamiltonians which are hybrid. These Hamiltonians contain DV qubit and CV qumode operator combinations such as, for instance, the controlled rotation in Eq. (20) corresponding to a dispersive light-matter interaction Hamiltonian. More generally, we may consider a unitary gate of the form,

$$U = \exp[i\lambda f(\sigma_x, \sigma_z) \otimes g(\hat{x}, \hat{p})], \quad (32)$$

acting on the composite system of a qubit and a qumode. In fact, in the context of combining the DV and CV approaches, it has been pointed out [187] that a suitable set

logical \bar{Z} Pauli operator, which are superpositions of delta peaks along the position axis as shown, the \bar{X} eigenstates are delta-peak superpositions along the momentum axis in the physical qumode's phase space. The small shift errors can then be shifts along x and p , and as these WH errors form a basis, *any* sufficiently small error may be corrected. This reasoning is similar to that for the standard CV qumode codes [183, 184, 185] against sufficiently large, stochastic shift errors in a single channel [186].

of elementary Hamiltonians, including the controlled rotations and additional uncontrolled displacements,

$$\{\sigma_x \hat{a}^\dagger \hat{a}, \sigma_z \hat{a}^\dagger \hat{a}, \hat{x}\}, \quad (33)$$

is, in principle, sufficient for universal quantum computation on qubits.¹⁶ Even earlier Lloyd considered a universal set containing only controlled displacements [180],

$$\{\pm \sigma_x \hat{x}, \pm \sigma_z \hat{x}, \pm \sigma_z \hat{p}\}. \quad (34)$$

Typically, in quantum optics, controlled rotations are easier to achieve than controlled displacements, as we started discussing at the end of Sec. 3.1 and shall exploit later [22]. Controlled displacements may be accessible in other systems using ion traps [188, 189, 190, 191] or squids [192].

There are two ways to understand the universality of the above Hamiltonian sets. One approach is based upon the decomposition,¹⁷

$$e^{iH_2 t} e^{iH_1 t} e^{-iH_2 t} e^{-iH_1 t} = e^{[H_1, H_2] t^2} + O(t^3). \quad (35)$$

So by applying the Hamiltonians H_1 and H_2 for some short time, we can also approximately implement the Hamiltonian $-i[H_1, H_2]$, provided the interaction times are sufficiently short.¹⁸ Now first of all it can be shown that using Eq. (35) and the elementary Hamiltonians of Eq. (34) one can generate through commutation any single-qubit, any single-qumode, as well as any qubit-qumode unitary [180]. The extra two-qubit and two-qumode entangling gates in order to complete the universal sets for DV and CV universality, respectively, are then achieved through the following commutators,

$$-i[\sigma_z^{(1)} \hat{x}, \sigma_z^{(2)} \hat{p}] = \sigma_z^{(1)} \sigma_z^{(2)} / 2, \quad (36)$$

$$-i[\sigma_z \hat{x}_1, \sigma_x \hat{x}_2] = 2 \sigma_y \hat{x}_1 \hat{x}_2, \quad (37)$$

respectively. Here, the superscripts and subscripts denote operators acting upon one of the two qubits or qumodes. In other words, the C_Z -gates of the sets in Eq. (10) and Eq. (12) can be enacted *approximately* by applying some of the elementary Hamiltonians in Eq. (34). However, there is a crucial difference between the above two commutators. The commutator in Eq. (36) commutes with the elementary Hamiltonians from which it is built, whereas the commutator in Eq. (37) does not. As a consequence, in the latter case, the decomposition formula in Eq. (35) is indeed only an approximation that requires infinitesimally small interaction periods. However, since $-i[\sigma_z^{(1)} \hat{x}, \sigma_z^{(2)} \hat{p}]$ commutes with $\sigma_z^{(1)} \hat{x}$ and $\sigma_z^{(2)} \hat{p}$, and all higher-order commutators vanish as well, the two-qubit C_Z -gate according

¹⁶ note that compared to the discussion on universal sets for DV and CV quantum computation in Sec. 2.3.1, we are now writing a universal set in terms of elementary Hamiltonians instead of elementary gates.

¹⁷ using the well-known Baker-Campbell-Hausdorff formula $e^A e^B = e^{A+B} e^{[A, B]/2} + O([A, [A, B]], [[A, B], B])$ and so $e^{\pm iH_2 t} e^{\pm iH_1 t} = e^{\pm i(H_1 + H_2)t} e^{-[H_2, H_1]t^2/2} + O(t^3)$.

¹⁸ this is the same asymptotic, approximate model for universal quantum computation as it was used for discrete [193] and continuous [8] variables on their own.

to Eq. (35) with Eq. (36) no longer depends on small interaction times. Instead we obtain the *exact* formula,

$$e^{i\sigma_z^{(2)} \hat{p} t} e^{i\sigma_z^{(1)} \hat{x} t} e^{-i\sigma_z^{(2)} \hat{p} t} e^{-i\sigma_z^{(1)} \hat{x} t} = e^{i\sigma_z^{(1)} \sigma_z^{(2)} t^2 / 2}. \quad (38)$$

This observation leads us to an alternative way of understanding how the hybrid gates of Eq. (34) can be used to achieve universal quantum computation on qubits. In particular, a two-qubit entangling gate of sufficient strength (i.e., $t^2 \sim 2\pi$) is then possible without direct interaction between the two qubits; a single qumode subsequently interacting with each qubit would rather mediate the qubit-qubit coupling – as a kind of *quantum bus* (so-called qubus [192, 194], see Fig. 3.3.2). The sudden exactness of the gate sequence can be explained by interpreting it as a controlled geometric phase gate [187, 195].

So even though the original hybrid scheme of Lloyd [180] achieves universality using a finite gate set, it appears unrealistic to switch between the elementary Hamiltonians over arbitrarily short time. Accomplishing the universal gates and hence the Hamiltonian simulation exactly over a finite number of steps, as described by Eq. (38), is thus an essential extension of these hybrid approaches.

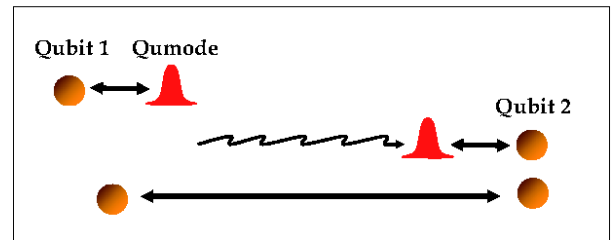


Figure: 3.3.2 A quantum optical illustration of the qubus principle. A CV probe pulse (qumode) subsequently interacts with two matter qubits. After a sequence of interactions an entangling gate between the two qubits can be mediated through the qubus. Compare this with the previous entanglement distributor in Fig. 3.2.2.

Let us finally note that the two-qumode C_Z gate, as discussed in Sec. 2.3.1, of course, can be implemented directly using beam splitters and squeezers, independent of a supposed asymptotic scheme based on Eq. (35) with Eq. (37). Such a simple realization, however, is typically not available for qubits. Therefore, the exact qubus-mediated two-qubit entangling gate construction here may turn out to be very useful. In Sec. 3.3.5, we shall discuss optical qubus schemes, similar to Fig. 3.3.2, utilizing controlled rotations obtainable from strong or weak nonlinear interactions.

3.3.3. Nonlinear resources and linear operations

The GKP scheme [10] is in some sense the CV counterpart to the DV KLM scheme [11]. The essential technique

exploited in both schemes is to induce a nonlinearity by means of measurements and to create a highly sophisticated, nonlinear ancilla state offline. This saves one from directly applying nonlinearities online. Conceptually, the essence of KLM and GKP is to combine an abstract model of measurement-based quantum computation with the notion of measurement-induced nonlinearities.

Similar to the discussion in Sec. 2.3, the measurement-based approaches can be divided into those based on quantum teleportation involving a nonlocal measurement and into cluster-based schemes requiring only local measurements with all entangling operations done offline prior to the actual computation. In this sense, KLM is teleportation-based, whereas GKP is cluster-based (though the original GKP scheme was not presented as a cluster-based scheme, but can be recast correspondingly [196]).

In order to obtain the necessary non-Clifford gate on the logical qubit through a non-Gaussian operation on the physical qumode (recall the discussion around Fig. 3.3.1), GKP propose to produce an approximate version of the cubic phase state offline, $D_3(\kappa)|p=0\rangle = e^{i\kappa\hat{x}^3}|p=0\rangle = \int dx e^{i\kappa x^3}|x\rangle$, using Gaussian two-mode squeezed state resources and photon number measurements (see Fig. 3.3.3). The resulting cubic phase state is then sufficient to accomplish the cubic phase gate $D_3(\kappa)$ and to apply it to an arbitrary input state $|\psi\rangle$ through linear operations including homodyne detections (see Fig. 3.3.4). The circuit in Fig. 3.3.4 with all gates performed offline can be interpreted as a CV cluster computation on a non-Gaussian cluster state, in which case homodyne detections are sufficient for universality [196].

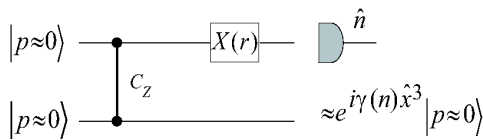


Figure: 3.3.3 The GKP approach for creating a cubic phase state [10] using linear, Gaussian resources and DV photon counting measurements. The Gaussian resource state, emerging from two momentum-squeezed states and the CV version of the controlled Z gate, $C_Z = e^{2i\hat{x}_1 \otimes \hat{x}_2}$, is a two-mode squeezed state up to a local Fourier rotation; $X(r) = e^{-2i\hat{r}\hat{p}}$ is a WH operator with fixed and sufficiently large r (much larger than the resource squeezing parameter). The circuit as drawn is reminiscent of an elementary step in a CV cluster computation involving a nonlinear measurement onto the displaced number basis $\{X^\dagger(r)|n\rangle\}$ [196].

The approximate cubic phase state in Fig. 3.3.3 will depend on the measurement result n , $e^{i\gamma(n)\hat{x}^3}|p=0\rangle$, and so for the desired cubic phase state, phase-free squeezing corrections are needed, $\hat{S}^\dagger[t(n)]e^{i\gamma(n)\hat{x}^3}\hat{S}[t(n)] = e^{i\kappa\hat{x}^3}$ with $t(n) = [\kappa/\gamma(n)]^{1/3}$ [196].

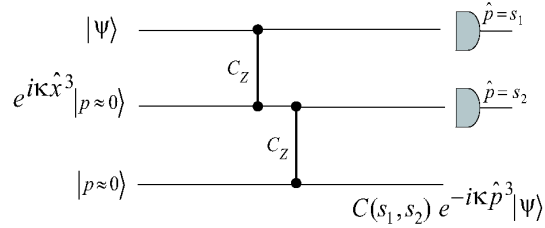


Figure: 3.3.4 Using an offline prepared cubic phase state $e^{i\kappa\hat{x}^3}|p=0\rangle$ in order to perform the cubic phase gate $e^{-i\kappa\hat{p}^3}$ on an arbitrary state $|\psi\rangle$ using linear, Gaussian operations. The final, Gaussian correction step to undo the operator $C(s_1, s_2)$ depending on the homodyne results s_1 and s_2 involves displacements, rotations, and squeezers because of the commuting properties of the cubic gate which is non-Gaussian/non-Clifford and so does not preserve the WH group under conjugation [197].

There is actually a CV scheme which appears to be an even closer analogue of KLM, as it is also teleportation-based using CV Bell measurements [127] on non-Gaussian resource states [197]. In fact, we could as well interpret the scheme in Fig. 3.3.4 as a teleportation-based scheme. In this case, only the entangling gate C_Z acting upon the second and third rails of the quantum circuit in Fig. 3.3.4 would be performed offline prior to the C_Z on the first and second rails. This way the C_Z on the upper two rails together with the two homodyne detections can be interpreted as a collective, homodyne-based CV two-mode Bell measurement on an input state $|\psi\rangle$ and one half of a non-Gaussian resource state which is the cubic phase state coupled to a momentum-squeezed state through a CV C_Z gate. This resource then is actually equivalent to a two-mode squeezed state with one mode subject to a cubic phase gate (up to a local Fourier transform), as the C_Z gate and the cubic gate $D_3(\kappa)$ commute.

Eventually, we may describe the protocol in terms of standard CV quantum teleportation where a nonlinearly transformed offline two-mode squeezed state is used as an EPR channel for CV quantum teleportation. In the case of a cubic offline resource, the online correction operations during the teleportation process will be quadratic containing squeezers and displacements; a quartic offline resource such as a self-Kerr transformed two-mode squeezed state leads to cubic corrections [197]. However, there are various ways how to incorporate a desired gate operation into a CV quantum teleportation scheme (see Fig. 3.3.5). As long as only linear (but collective two-mode), homodyne-based measurements on an input mode and one mode of a nonlinear, non-Gaussian resource state are permitted, the degree of the correction operations is always one order less than the order of the desired gate. As a result, only the cubic gate can be realized using cubic resources and Gaussian measurements and corrections; a quartic gate requires linear measurements, but cubic corrections which, of course, may also be implemented using cubic offline resources.

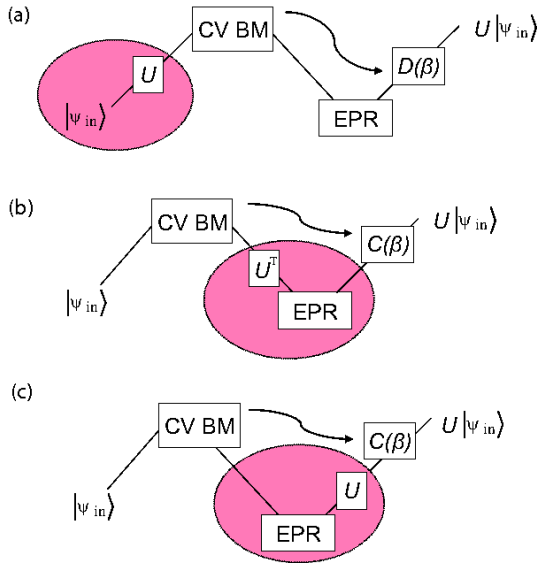


Figure: 3.3.5 Teleportation-based implementation of a nonlinear, unitary gate U such as the cubic phase gate or a quartic Kerr-type gate. In all schemes, the online operations are: a two-mode, homodyne-based CV Bell measurement ‘CV BM’ and the measurement-dependent corrections using displacements $D(\beta)$ or displacements and additional operations $C(\beta)$ with a Hamiltonian degree of one order lower than the nonlinearity order of U ; the offline resource state is a nonlinearly transformed, Gaussian two-mode squeezed ‘EPR’ state, except in the trivial, teleportation-based scheme (a) where the input state $|\psi_{\text{in}}\rangle$ is first transformed according to the desired gate U and then teleported; as $|\psi_{\text{in}}\rangle$ may be arbitrary and unknown, the scheme (a) is not a valid offline-scheme and would require an online gate U acting upon $|\psi_{\text{in}}\rangle$. The schemes (b) and (c) are similar, only differing in the particular EPR-mode to which the nonlinear gate U is applied offline. The nonlinear resources are always indicated by a red circle; only for the case of a cubic gate U are all online operations Gaussian. Up to local Fourier transforms and squeezers, the scheme of Fig. 3.3.4 is a special example of that in (b). Of course, we may also consider combinations of (a), (b), and (c).

Once a quartic self-Kerr-type gate can be implemented using CV quantum teleportation [e.g. like in Fig. 3.3.5 (b) or (c)], such a scheme could be applied to two qubits, as shown in Fig. 2.3.1. Together with the two beam splitters (and taking into account the finiteness of the resource squeezing for teleportation), this results in an *approximate, unconditional, and thus deterministic* realization of a two-qubit C_Z gate, as opposed to the perfect, nondeterministic implementation of KLM [11]. However, note that the correction operations before the second beam splitter are still cubic and so would require further nonlinear processing.

The scheme of Fig. 3.3.4 is a special example of the scheme (b) in Fig. 3.3.5. In the general case of Fig. 3.3.5 (b), the gate U to be implemented can be arbitrary and need not be diagonal in the x -basis. For the cluster-type circuit in Fig. 3.3.4, however, it is useful that the entangling gates C_Z and the desired cubic gate operation D_3

are all diagonal in x and hence commute.¹⁹ Starting with a two-mode squeezed state $\sum_{n=0}^{\infty} c_n |n, n\rangle_{1,2}$ with $c_n \equiv \tanh^n r / \cosh r$ for a squeezing parameter r , we may apply the transfer formalism for standard CV quantum teleportation [198] and extend it to the present case of gate teleportation. Then we obtain the conditional state after the Bell projection of the input qumode and qumode 1 onto $\hat{T}(\beta) \equiv |\Phi(\beta)\rangle\langle\Phi(\beta)|$ for the CV Bell basis $|\Phi(\beta)\rangle \equiv [\hat{D}(\beta) \otimes \mathbf{I}] \sum_{m=0}^{\infty} |m, m\rangle / \sqrt{\pi}$,

$$\hat{T}_{\text{in},1}(\beta) \left\{ |\psi_{\text{in}}\rangle \otimes \left[(U_1^T \otimes \mathbf{I}_2) \sum_{n=0}^{\infty} c_n |n, n\rangle_{1,2} \right] \right\}, \quad (39)$$

corresponding to a conditional state of qumode 2 alone,

$$\sum_n \frac{c_n}{\sqrt{\pi}} |n\rangle \sum_m U_{mn}^T \langle m | \hat{D}^\dagger(\beta) | \psi_{\text{in}} \rangle = \mathcal{D} U \hat{D}^\dagger(\beta) | \psi_{\text{in}} \rangle, \quad (40)$$

with the ‘distortion operator’ $\mathcal{D} \equiv \sum_n c_n |n\rangle\langle n| / \sqrt{\pi}$ and the matrix elements $U_{mn}^T \equiv \langle m | U^T | n \rangle = \langle n | U | m \rangle$. After a suitable correction operation $C(\beta)$, the input state is ‘transferred’ onto the output state $\hat{T}_U(\beta) | \psi_{\text{in}} \rangle$ with

$$C(\beta) \mathcal{D} U \hat{D}^\dagger(\beta) \equiv C(\beta) \mathcal{D} C^\dagger(\beta) U \equiv \hat{T}_U(\beta), \quad (41)$$

where the first equality defines the right correction operation $C(\beta)$ depending on the gate U and its commuting properties with the displacement operator, $U \hat{D}^\dagger(\beta) = C^\dagger(\beta) U$. The degree of $C^\dagger(\beta)$ will always be one order lower than the order of U [197]. In the limit of infinite squeezing, we obtain the desired gate teleportation. For finite squeezing r , there will be a distortion resulting in a nonunit-fidelity gate, $F = \int d^2\beta |\langle \psi_{\text{in}} | U^\dagger \hat{T}_U(\beta) | \psi_{\text{in}} \rangle|^2 < 1$. We shall look at the scheme in Fig. 3.3.5 (b) as well as that in Fig. 3.3.5 (a) from a different perspective in the following section.

Further refinements and proposals related with GKP can be found in Refs. [199,200]. An alternative approach to implementing a cubic phase gate relies upon potentially more accessible non-Gaussian resources such as Fock-state ancillae [125]. Similarly, nonlinear Fock-state ancillae may be exploited in order to achieve nonlinear Fock-state projection measurements using linear, Gaussian measurements in form of two homodyne detectors after a beam splitter [201] (see Fig. 3.3.6). More specifically, postselecting the homodyne results around zero leads to $\hat{T}_{\text{in},1}(\beta) \approx$

¹⁹ in the scheme of Fig. 3.3.5 (c), an arbitrary gate U , instead of applying it at the very end of CV quantum teleportation, can just be commuted through the final teleportation displacement operation, $U D(\beta) = C(\beta) U$, with $C(\beta)$ a correction operation of one order lower than the order of U and U applied offline to the EPR state [197]. Similarly, the scheme of Fig. 3.3.5 (b) may be understood by rewriting the offline transformed, maximally entangled EPR state of (c), $(\mathbf{I} \otimes U) | \text{EPR} \rangle = (U^T \otimes \mathbf{I}) | \text{EPR} \rangle$, in the limit of infinite squeezing; for the finite-squeezing case, see main text.

$0\rangle|m\rangle_1 \propto \text{in}\langle m|$. Projecting onto this two-mode basis corresponds to applying a symmetric beam splitter transformation followed by x and p homodyne detections like for the CV Bell measurement in CV quantum teleportation [127], as in Fig. 3.3.6.

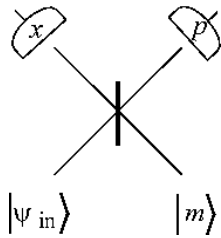


Figure: 3.3.6 Nonlinear (destructive) projection of an input state $|\psi_{\text{in}}\rangle$ onto the Fock state $|m\rangle$ through x and p homodyne detections and postselection using a beam splitter and an ancilla Fock state $|m\rangle$ [201].

The proposal of Ref. [201] can be used to realize various quantum information tasks, including the implementation of a NSS gate. However, the need for postselection renders this approach again fairly inefficient. For example, for the NSS gate, fidelities $F > 0.9$ are obtainable at success probabilities $< 10^{-4}$. Nonetheless, in general, preparing nonlinear ancilla resource states offline,²⁰ possibly in a nondeterministic fashion, but with reasonable fidelities, offers a promising approach to universal quantum information processing, as the online operations in this case can be restricted to only linear ones. These linear operations may include squeezing corrections which could also be efficiently implemented, provided high-quality CV cluster states are available. Such linear, universal resource states will be part of the discussion in the following section.

3.3.4. Linear resources and nonlinear operations

The circuit in Fig. 3.3.4 describes a protocol in which a nonlinear cubic phase gate is implemented using an offline cubic phase state and online Gaussian operations. In order to accomplish the gate $D_3(\kappa)$, a cubic state of the form $D_3(\kappa)|p=0\rangle$ is needed. So there should be a sufficient supply of cubic states such that after injecting these into a CV Gaussian cluster state, sets of cubic gates can be applied through homodyne detections whenever needed during a computation [56, 196, 203].

A canonical version of a Gaussian CV cluster state [204, 136] is shown in Fig. 3.3.7. An elementary cluster computation step between two qumodes of the cluster corresponds to the circuit in Fig. 3.3.8.

²⁰ the degree of nonlinearity and non-Gaussianity of which may even be tuned in a heralded state generation scheme [202].

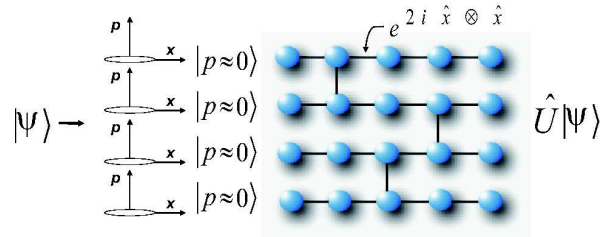


Figure: 3.3.7 An approximately universal, Gaussian CV cluster state built from momentum-squeezed states of light and Gaussian, CV versions of the C_Z gate, $e^{2i\hat{x}\otimes\hat{x}}$. An arbitrary multi-mode state $|\psi\rangle$ attached from the left can then be universally processed through local projection measurements of the individual qumodes of the cluster such as homodyne and photon number measurements [56]. The output state $\hat{U}|\psi\rangle$ of the cluster computation will appear on the most right column in the remaining, undetected qumodes.

The gates in front of the x -homodyne detector in the circuit of Fig. 3.3.8 can be absorbed into the measurement apparatus such that instead of measuring the observable \hat{x} the projection is onto the rotated p -basis $\{D^\dagger|p\rangle\}$ measuring the observable $D^\dagger\hat{p}D$. This way we can apply any gate $D = e^{if(\hat{x})}$ to an arbitrary input state teleported into the upper rail in Fig. 3.3.8, that is into one or, in the multi-mode case, several qumodes of the most left column in Fig. 3.3.7. Further application of such elementary steps, by measuring out the other qumodes in the CV cluster state beginning from the left in Fig. 3.3.7, may lead to, in principle, universal quantum computation on multi-qumode states in the approximate, asymptotic sense as discussed in Sec. 2.3.1 [56]. A Fourier transform can be performed through the cluster at any step in order to switch between \hat{x} and \hat{p} gates. To complete the universal set in Eq. (12), the two-qumode gate C_Z is obtainable through the vertical wires in Fig. 3.3.7, so the cluster must be at least two-dimensional. The total evolution of the input is completely controlled by the measurements with the cluster state prepared offline prior to the computation.

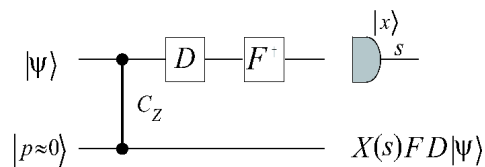


Figure: 3.3.8 Elementary step of a CV cluster computation. The desired gate operation $D = e^{if(\hat{x})}$ and the inverse Fourier transform F^{-1} can be absorbed into the measurement apparatus such that a projection of the upper qumode onto the basis $\{D^\dagger|p\rangle\}$ with result s leaves the lower qumode in the desired output state up to a Fourier transform and a WH correction $X(s)$. Compare this with the analogous qubit circuit in Fig. 2.3.5.

Any multi-mode LUBO as described by Eq. (1) can be performed on an arbitrary multi-mode state through homodyne detections alone. An additional *nonlinear measurement such as photon counting is needed in order to be able to realize gates of cubic or higher order*. In this case, the basis choice of a measurement in one step would typically depend on the outcomes of the measurements in the previous steps. In contrast, in the all-homodyne-based scenario for LUBOs, no such feedforward is required and all measurements may be conducted in parallel – a feature known as Clifford parallelism for qubit cluster computation.

It has been proven that a linear four-mode cluster state is sufficient to achieve an arbitrary single-mode LUBO (see Fig. 3.3.9); an arbitrary N -mode LUBO is possible using a finite, two-dimensional CV cluster state of $\sim N^2$ qumodes [205]. In this case, no more asymptotic evolutions with infinitesimal, elementary steps must be considered, but rather combinations of beam splitter and single-mode squeezing gates of appropriate strength. Such cluster-based LUBOs circumvent the complication of online squeezing of, especially, fragile non-Gaussian states, since all squeezing gates are performed offline on the Gaussian cluster state. Provided enough squeezing is available to create the cluster states [136,206,207,196], this approach may also be used to *realize the necessary squeezing corrections for nonlinear gate implementations*, as discussed in the preceding section. The single-mode LUBO scheme was recently implemented experimentally [208,209]. More experiments on the creation of various CV cluster-type states and the offline implementation of CV C_Z -type gates are presented in Refs. [210,211] and Ref. [26], respectively.

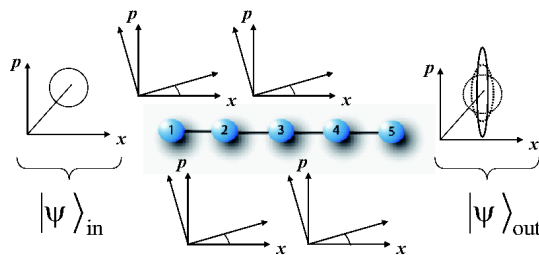


Figure: 3.3.9 Universal single-mode LUBO. After attaching an arbitrary single-qumode input state to a linear four-mode cluster state (qumodes 2-5), appearing in qumode 1, four elementary steps, involving four quadrature homodyne detections on qumodes 1-4 with suitably chosen local-oscillator quadrature angles, are sufficient to obtain approximately any LUBO-transformed output state in qumode 5, provided the squeezing in the linear cluster state is sufficiently large. The C_Z -attachment of the input state and the two homodyne detections on qumodes 1 and 2 can be replaced by a CV Bell measurement on the input mode and the most left mode, qumode 2, of the cluster [205]. The input state is depicted as a Gaussian coherent state only for illustration. Most significantly, the CV Bell measurement can also be used to teleport non-Gaussian input states into the four-mode cluster for universal, linear processing.

In comparison to the scheme in Fig. 3.3.4, which employs a suitable nonlinear resource state and linear operations, the GKP approach for realizing a cubic phase gate can also be directly incorporated into a CV cluster computation [196]. In this case, the offline resource state remains Gaussian and thus unconditionally producible, while some of the online operations must then become nonlinear (see Fig. 3.3.10). In order to obtain a desired cubic gate of any given strength κ , as before, additional squeezing corrections are needed. However, this time, also the squeezing corrections are performed through cluster computation, since any squeezing gate is available by propagating the relevant state through a horizontal, linear four-mode wire (see Fig. 3.3.11).

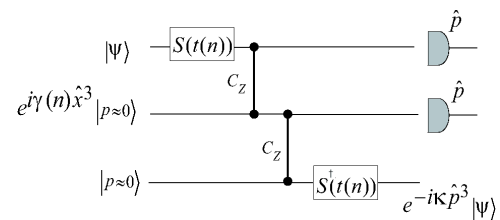


Figure: 3.3.10 Incorporating the GKP scheme into a CV cluster computation. The resource state remains Gaussian, the measurements are CV homodyne detections and DV photon number measurements to teleport the cubic phase state into the middle rail. The initial cubic phase state depends on the measurement outcome n and extra squeezing corrections S are needed to obtain a cubic gate of any desired strength κ . Compared to Fig. 3.3.4, the n -dependent squeezing corrections S are here to be done through the cluster (Fig. 3.3.11); the additional p -dependent squeezing and WH corrections $C(s_1, s_2)$ can also be incorporated into the cluster computation and are not shown for simplicity.

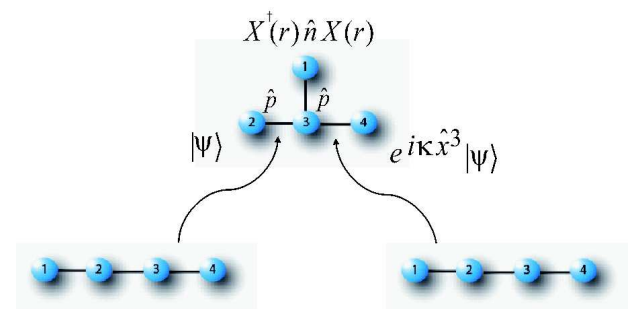


Figure: 3.3.11 Full CV cluster implementation of a cubic phase gate. The extra linear cluster states are needed to realize the necessary squeezing corrections which depend on the photon number measurement result. As the desired cubic gate is non-Gaussian, the order of the measurements matters and the number measurement has to be done first. This implementation using linear and nonlinear measurements on a Gaussian state is conceptually different from that illustrated in Fig. 3.3.4 where the resource state is non-Gaussian and all online operations are linear.

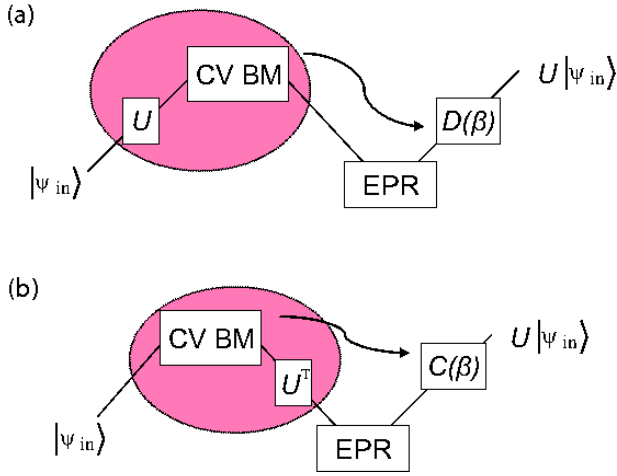


Figure: 3.3.12 Gate teleportation using collective, nonlinear projection measurements on an input state $|\psi_{\text{in}}\rangle$ and one half of a Gaussian two-mode squeezed state that serves as an EPR source; (a) compared to Fig. 3.3.5 (a), the nonlinear gate U is absorbed into the Bell measurement; similarly, (b) compared to Fig. 3.3.5 (b), the nonlinear gate U^T is absorbed into the Bell measurement. The nonlinear elements are again indicated by the red circles, this time corresponding to suitable projective measurements.

Formally, we may also interpret some of the schemes in Fig. 3.3.5 as gate teleports for arbitrary qumode gates U using nonlinear operations on linear resources, where a Gaussian two-mode squeezed state is used as an EPR source and a nonlinearly modified, two-mode Bell measurement is employed (see Fig. 3.3.12). For example, the scheme in Fig. 3.3.12 (a) can be formally described as

$$\hat{H}_{\text{in},1}^{(U)}(\beta) \left(|\psi_{\text{in}}\rangle \otimes \sum_{n=0}^{\infty} c_n |n, n\rangle_{1,2} \right) = \mathcal{D}\mathcal{D}^\dagger(\beta)U|\psi_{\text{in}}\rangle, \quad (42)$$

using the definitions of Sec. 3.3.3 and $\hat{H}^{(U)}(\beta) \equiv (U^\dagger \otimes \mathbf{1})\hat{H}(\beta)(U \otimes \mathbf{1})$, describing a projection onto the basis $\{(U^\dagger \otimes \mathbf{1})|\Phi(\beta)\rangle\}$ for a fixed U . As such collective, nonlinear measurements are not known to be experimentally available, there seems to be no advantage of the schemes in Fig. 3.3.12 besides the conceptual insights they provide. The scheme in Fig. 3.3.12 (a) does not require any correction operations other than displacements, because it is equivalent to that in Fig. 3.3.5 (a), where the gate U is trivially applied through teleportation by first performing U on $|\psi_{\text{in}}\rangle$ and then teleporting $U|\psi_{\text{in}}\rangle$ using standard CV quantum teleportation.

Concluding this section, we can say that it depends to a large extent on the experimental implementability of nonlinear measurements such as photon number resolving detections whether more advanced or ultimately universal, optical quantum information protocols can be realized in the laboratory. If, similar to the quantum-state tunability between offline Gaussian and non-Gaussian resource states [202], also the online operations for measurement-

based approaches, i.e., the quantum-state measurements, could be tuned over a sufficient range of linear CV and nonlinear DV POVMs [212], efficient experimental realizations may then be possible in the near future. In this case, the offline resource states may be, for example, Gaussian CV cluster states which can be built unconditionally from squeezed light using beam splitters. However, finite-squeezing-induced imperfections will then require some additional nonlinear element for quantum error correction. Alternatively, instead of attempting to perform full computations over CV cluster states at a precision that decreases linearly with the size of the computation (number of measurement steps) for a given initial squeezing variance [196], one may just use Gaussian ancilla states, nonlinearly measured online or offline, for implementing particularly difficult gates such as the NSS gate on DV photonic states and do the simple gates on dual-rail encoded qubits directly in the standard circuit approach.

3.3.5. Weakly nonlinear operations

In this section, we shall now consider schemes where a nonlinear element is part of an optical quantum protocol in form of some nonlinear interaction, but this nonlinearity is no longer required to be sufficiently strong. Recall the discussion in Sec. 3.3.2 on hybrid Hamiltonians. Using an ancilla qumode as a quantum bus that mediates a nonlinear interaction between two qubits, as depicted in Fig. 3.3.2, we can construct universal two-qubit gates by means of rotations or displacements of the qumode conditioned upon the state of the respective qubit. Sequences of such qubit-qumode interactions may then result in an effective two-qubit entangling gate after the qumode is finally measured out or when the qumode automatically disentangles from the two qubits, as, for instance, described by the sequence in Eq. (38). In this example, though the ancilla qumode and each qubit do become entangled during the gate sequence, an initially unentangled qumode will be again unentangled at the end, as can be easily understood from the right-hand-side of Eq. (38).

In the quantum optical regime, using either dispersive light-matter interactions or all-optical Kerr-type interactions, qubit-controlled qumode rotations enable one to perform various tasks from projecting onto the complete DV photonic Bell basis to implementing photonic two-qubit entangling gates, employing either DV (threshold) photon detectors [16], CV homodyne detectors [17, 18, 19, 20], or no detectors at all [21, 22].

In this section, we shall briefly discuss the *measurement-free approach*. Schemes where the qumode ancilla is eventually measured are particularly useful for quantum communication and will be considered in the next section. The measurement-based and measurement-free schemes can differ in their controlled, qubit-qumode gate sequences and also in the scaling of the nonlinear element with photon losses for the realistic case of imperfect, lossy quantum gates and communication channels.

Most importantly, the qubit-qumode interactions, realizable, for instance, through dispersive light-matter couplings in a CQED setting such as the “single-atom dispersion” discussed in Sec. 3.1, are typically fairly weak. Thus, the resulting controlled gates produce conditional phase angles θ which are initially too small to be useful, $\theta \sim 10^{-2}$ or smaller. However, the hybrid qubit-qumode systems are designed such that a sufficiently intense qumode beam leads to an effectively enhanced interaction. On the other hand, qumode ancilla pulses carrying too many photons, when temporarily entangled with a low-dimensional qubit, are very likely to transfer photons containing which-path qubit information into the environment. Therefore, the hybrid entangled states and the hybrid gates become more sensitive to photon losses.

Let us write a sequence similar to that in Eq. (38) in terms of quantum optical displacement operations, each depending on a qubit Pauli operator,

$$\hat{D} \left[i\beta_2 \sigma_z^{(2)} \right] \hat{D} \left[\beta_1 \sigma_z^{(1)} \right] \hat{D} \left[-i\beta_2 \sigma_z^{(2)} \right] \hat{D} \left[-\beta_1 \sigma_z^{(1)} \right] \quad (43)$$

$$= \exp \left[2i \operatorname{Re}(\beta_1^* \beta_2) \sigma_z^{(1)} \sigma_z^{(2)} \right].$$

These controlled displacements, acting upon the composite system of two qubits and one qumode, generate a two-qubit entangling gate, as discussed before. The two-qubit gate relies upon a phase shift that is acquired by a qumode whenever it goes along a closed loop in phase space. This geometric phase depends on the area of the loop and not on its form [187]. It comes from the extra phase factor in $\hat{D}(\beta_1)\hat{D}(\beta_2) = \exp[i \operatorname{Im}(\beta_1\beta_2^*)] \hat{D}(\beta_1 + \beta_2)$. Note that the qumode may start in *any* state.

In quantum optics, the controlled displacement operations of Eq. (43) are not really available. Two-qubit geometric phase gates directly implemented from controlled rotations through dispersive light-matter interactions result in final states with a qumode still entangled with the two qubits [145]. The extra dephasing from this effect, however, can be completely avoided by simulating every controlled displacement in Eq. (43) through yet another sequence of controlled rotations and uncontrolled displacements [22],

$$\hat{D}(\alpha \cos \theta) \hat{R}(\theta \sigma_z) \hat{D}(-2\alpha) \hat{R}(-\theta \sigma_z) \hat{D}(\alpha \cos \theta)$$

$$= \hat{D}(2i\alpha \sin \theta \sigma_z), \quad (44)$$

using Eq. (20).

In order to obtain a maximally entangling two-qubit gate, we need $\beta_1\beta_2 = \pi/8$ (assuming real β_1 and β_2) and so $2\alpha \sin \theta = \sqrt{\pi/8} \approx 0.6$ (assuming real α). For small θ , this means that α must be sufficiently large such that $\alpha\theta \sim 1$. For instance, when $\theta \sim 10^{-2}$, phase-space displacements corresponding to mean photon numbers of the order of 10^4 are required. For stronger interactions θ , correspondingly smaller displacements are enough. Note that the strength of the displacements in Eq. (44), inserted into Eq. (43), determines the effective enhancement of the nonlinear two-qubit gate, as the qumode starts in an arbitrary state.

The deterministic, measurement-free gates described here could be, in principle, used directly in a DV quantum computation, utilizing either matter qubits dispersively interacting with optical ancilla qumodes or photonic qubits weakly nonlinearly coupled to photonic ancilla qumodes. Alternatively, these gates may provide a mechanism for growing DV qubit cluster states in an efficient, deterministic fashion; for certain simple (though non-universal) graph states such as linear or star (GHZ-type) graphs, the qumode may interact as little as two times with each qubit to build up the graph [213]. This is different from the nondeterministic, standard linear-optics approaches [52,53,54,55], but similar to the unconditional gate teleportations using Gaussian ancilla cluster resources discussed in the preceding sections.

However, whereas the fidelity of even an ideal implementation with CV cluster states is fundamentally limited by the finite squeezing of the cluster states and other imperfections in the extra non-Gaussian ancilla states or measurements, the ideal weak-nonlinearity-based protocol would, in principle, achieve unit fidelity at unit efficiency. Of course, this only holds provided that the hybrid qubit-qumode interactions are perfect. Realistically, these interactions are very sensitive to photon losses, especially those with large α -paths in phase space like in Eq. (44) when θ is small, and so for every gate protocol, a careful loss analysis is needed [214,215]. In general, it will be useful to minimize the number of necessary interactions in a gate sequence. One possibility then would be to employ measurement-based entangling gates including postselection, rendering the quantum computational routines again nondeterministic [213,216]. The measurement-based approach is also preferred for quantum communication protocols when two spatially separated memory qubits are to be entangled over a distance. This will be discussed in the next section.

Let us finally mention that the concept of using a quantum bus has other advantages too. In general, photonic qubit or qumode ancillae may be employed to mediate interactions between non-nearest-neighbour signal qubits in a solid-state system [217,218,219,220,221,222]. In principle, this allows for universality and scalability when arbitrarily many signal qubits are added to the system. Two-qubit gates can then be performed for any pair and there is no need for two qubits to be so close together that individual addressing is no longer possible. The first qubus proposals were based upon both qubit signals and qubit ancillae, including, for instance, the well-known ion-trap proposal [194] with a phononic ion qubit mediating a gate between two internal two-level ion qubits. The more recent hybrid approaches as described here would rather use a photonic CV qumode ancilla serving as a quantum bus.

3.4. Hybrid quantum communication

Quantum communication over a distance as large as 1000 km or more is, in principle, possible by means of quan-

tum repeaters. As discussed in detail in Sec. 2.4, a quantum repeater operates by distributing entangled states over sufficiently short channel segments and connecting them through teleportation in combination with entanglement distillation. As the teleportation and distillation steps require local Bell measurements and entangling gates, with each repeater node effectively functioning as a small quantum computer, we shall in this section omit detailed discussions on the connection and distillation part of a repeater. For this purpose (Figs. 3.4.3 and 3.4.4), in principle, some of the quantum computational hybrid protocols of Sec. 3.3 could be used.

Our focus in this section is on the distribution of entangled qubit memory pairs between two neighboring repeater stations. There are various non-hybrid approaches for this of which some were presented in Sec. 2.4.²¹ Typically, in these entanglement distribution protocols, some form of local light-matter interaction is needed in order to transfer the quantum correlations encoded into the flying (optical) qubit/qumode systems that travel along the channel onto the local static qubit/qumode systems (which are typically either single electronic spin qubits or collective atomic spin qumodes placed in a cavity or just in free space, as discussed in Sec. 2.4).

A hybrid approach to entanglement distribution may work as illustrated in Fig. 3.2.2 or, alternatively, like the qubus scheme of Fig. 3.3.2. In either case, the qumode(s) should propagate through the lossy communication channel only once and any additional communication will be classical, for instance, for confirming a successful entanglement generation attempt among the neighboring parties. Focussing on a qubus-based repeater protocol like in Fig. 3.3.2, the measurement-free, entangling gate sequences of Sec. 3.3.2 and Sec. 3.3.5 are better suited for the local repeater operations, while a *measurement-based approach* with only one interaction of the qumode ancilla with each local qubit is optimal for the nonlocal entangled-state preparation. In this case, the measurement is needed in order to disentangle the qumode from the tripartite entangled qubit-qubit-qumode system and to project the two qubits onto a near-maximally entangled state. When photon losses in the channel are taken into account, the qumode detection scheme will typically include postselection of “good” measurement results.

Consider the qubus scheme of Fig. 3.3.2. After a first dispersive interaction, i.e., a controlled phase rotation of the qumode ancilla starting in a coherent state $|\alpha\rangle$ (α real) depending on the state of the first qubit [with initial state $(|0\rangle + |1\rangle)/\sqrt{2}$], the resulting hybrid qubit-qumode state has the form of Eq. (27) with, for example, $|\psi_0\rangle \equiv |\alpha\rangle$, $|\psi_1\rangle \equiv |\alpha e^{i\theta}\rangle$, and $\phi \equiv \alpha^2 \sin \theta$ in the orthogonal qumode

²¹ those non-hybrid approaches do not really combine DV and CV techniques according to our definition of hybrid schemes. However, recall that all these quantum repeater proposals do rely upon local quantum memories and hence local light-matter interfaces, rendering them “hybrid” according to the supposed standard definition of combined photon-atom systems.

basis of Eq. (26) [223]. We may represent this hybrid state by $|\Phi^+(\mu)\rangle \equiv \mu|u\rangle|0\rangle + \sqrt{1-\mu^2}|v\rangle|1\rangle$. Sending the qumode through a lossy fiber channel with amplitude transmission $\sqrt{\eta}$ then leads to a mixture of two different hybrid entangled qubit-qumode states [160],

$$F|\Phi^+(\mu)\rangle\langle\Phi^+(\mu)| + (1-F)|\Psi^+(\mu)\rangle\langle\Psi^+(\mu)|, \quad (45)$$

with $|\Psi^+(\mu)\rangle \equiv \mu|u\rangle|1\rangle + \sqrt{1-\mu^2}|v\rangle|0\rangle$ and an attenuated amplitude $\alpha \rightarrow \sqrt{\eta}\alpha$ throughout. Here the “fidelity” is $F \equiv [1 + e^{-(1-\eta)\alpha^2(1-\cos\theta)}]/2$ and the Schmidt coefficient is $\mu = \sqrt{1 + e^{-\eta\alpha^2(1-\cos\theta)}}/\sqrt{2}$. As this mixed entangled state is effectively written in a two-qubit basis, its entanglement can be quantified. Figure 3.4.1 shows the entanglement of formation [224] of the hybrid qubit-qumode state of Eq. (45) as a function of the initial qumode photon number α^2 for a 10 km fiber transmission. The trade-off between good initial entanglement and loss-induced decoherence for α too large ($\mu^2, F \rightarrow 1/2$) and, on the other hand, vanishing initial entanglement and only little decoherence for α too small ($\mu^2, F \rightarrow 1$) is clearly reflected in the entanglement.

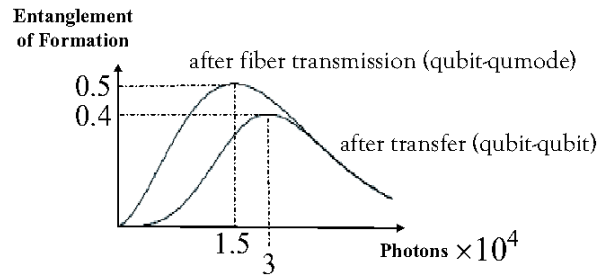


Figure 3.4.1 Entanglement of formation for the hybrid qubit-qumode states as a function of the mean photon number in the initial qumode coherent state after optical-fiber qumode transmission. Similarly, the entanglement of formation for the qubit-qubit states after the entanglement transfer through homodyne detection. Losses are 1.8 dB corresponding to roughly 10 km fiber transmission. Entanglement transfer postselection efficiency is 36 % and the local dispersive light-matter, qumode-qubit interactions are assumed to create phase shifts of the order of 10^{-2} .

The essence of the qubus scheme in Fig. 3.3.2 is that the noisy qubit-qumode entanglement after the imperfect channel transmission of the qumode is finally transferred onto the second qubit at the receiving station. This can be accomplished through a second dispersive interaction followed by a measurement on the qumode. Before the measurement, a second controlled qumode rotation then gives a tripartite entangled state of the two qubits and the qumode [160],

$$F|\Phi^+\rangle\langle\Phi^+| + (1-F)|\Phi^-\rangle\langle\Phi^-|, \quad (46)$$

with the pure tripartite states $|\Phi^\pm\rangle$ equal to

$$\frac{|\sqrt{\eta}\alpha\rangle|\phi^\pm\rangle}{\sqrt{2}} \pm \frac{e^{-i\phi}|\sqrt{\eta}\alpha e^{i\theta}\rangle|10\rangle}{2} + \frac{e^{i\phi}|\sqrt{\eta}\alpha e^{-i\theta}\rangle|01\rangle}{2}, \quad (47)$$

and the maximally entangled Bell states $|\phi^\pm\rangle = (|00\rangle \pm |11\rangle)/\sqrt{2}$.

For the final step of disentangling the qumode from the two qubits through measurement and projecting the two qubits onto an approximate version of $|\phi^+\rangle$ or also $(|10\rangle + |01\rangle)/\sqrt{2}$, there are various choices of which a homodyne detection is the experimentally most efficient option [223] (see Fig. 3.4.2). In this case, a discrimination of the states $\{|\sqrt{\eta}\alpha\rangle, |\sqrt{\eta}\alpha e^{\pm i\theta}\rangle\}$ in Eq. (47) along the x -axis will result in overlap errors depending on the effective distance of the Gaussian peaks that scales as $\sim \alpha\theta^2$ for small θ (see Fig. 3.1.3); hence α must be very large to compensate small θ and suppress the overlap errors (e.g. photon numbers of $\sim 10^8$ for $\theta \sim 10^{-2}$). As a result, the loss-induced decoherence becomes too large.

A better option is homodyne detection along p with peak distances $\sim \alpha\theta$. This scaling is the same as for the measurement-free schemes and still feasible with weak interactions θ . However, in this case, only those outcomes consistent with $|\sqrt{\eta}\alpha\rangle$ lead to an entangled two-qubit state and the conditional states corresponding to $\{|\sqrt{\eta}\alpha e^{\pm i\theta}\rangle\}$ must be discarded through postselection. There will then be a trade-off between pair creation efficiencies and fidelities, similar to the trade-off for the hybrid entanglement after transmission; and for the optimal transmission, the homodyne-based scheme will also not allow for a complete entanglement transfer from the hybrid to the two-qubit states (Fig. 3.4.1).

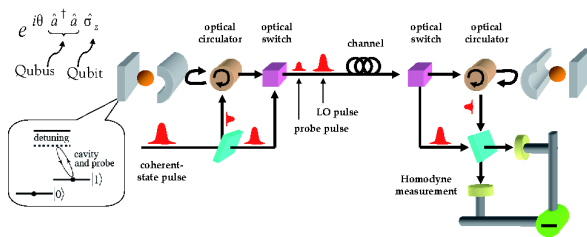


Figure: 3.4.2 Entanglement distribution in a hybrid quantum repeater using dispersive light-matter interactions and homodyne detection [223]. “LO” stands for “local oscillator”.

An interesting alternative is to replace the homodyne detection by a non-Gaussian POVM for USD of coherent states (see Fig. 2.2.3). In this case, an error-free identification of $|\sqrt{\eta}\alpha\rangle$ in Eq. (47) is possible, completely eliminating bit-flip errors [160]. The remaining phase-flip errors caused by photon losses may be minimized and thus fidelities for given success probabilities maximized through optimal USD [160], attainable, for instance, by means of

photon number resolving detectors and using two probe pulses [225]. Other non-Gaussian POVMs such as CSS state projections can be considered [226] as well as homodyne detections on squeezed-state instead of coherent-state qumode ancillae [227]. All these variations have in common that they achieve tunability of the fidelity against the success probability including near-unit fidelities at reasonable probabilities of success, a feature that is very useful for a full quantum repeater architecture.

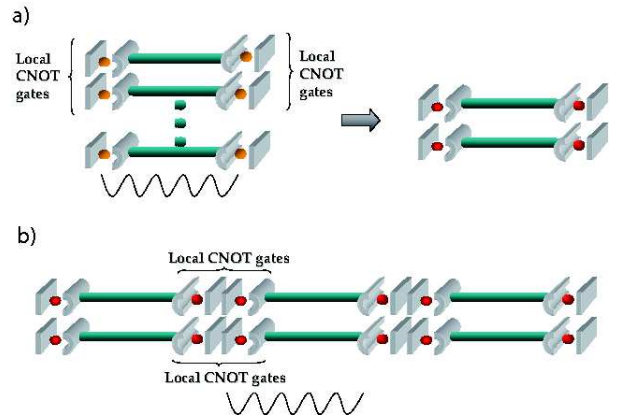


Figure: 3.4.3 Ingredients of a hybrid quantum repeater. (a) Distillation of better entangled states from a supply of noisy entangled states using local entangling gates such as C_Z or $CNOT$, qubit measurements, and classical communication. (b) Connecting the distilled entangled states through entanglement swapping using local $CNOT$ gates, qubit measurements, and classical communication.

The full hybrid quantum repeater is shown in Fig. 3.4.3. The local entangling gates for entanglement distillation and swapping could also be performed using dispersive light-matter interactions. The local qumode ancillae in this case can be prepared independent of the channel distances. Therefore arbitrarily intense qubus amplitudes are possible, provided other imperfections such as local dissipations and coupling inefficiencies in the CQED part of the repeater nodes can be suppressed [145] (see Fig. 3.4.4). In this case, CV homodyne measurements can result in sufficiently good state discrimination for the local parity gates (in a measurement-based implementation for the local gates), while the nonlocal qumode ancillae that interact with two spatially separated qubits and hence must be sufficiently weak could still be detected through non-Gaussian USD by means of DV photon number measurements.

The distances between repeater stations are 10-30 km, almost directly compatible with classical optical networks. A naturally given advantage of the hybrid, photonic flying-qumode-based quantum repeater over the photonic flying-qubit-based approaches is that it does not require long-distance interferometry. Nonetheless, both on the experi-

mental and on the theoretical side there are still open issues such as efficient local memory transfers (e.g. from electronic to nuclear spins, recall the discussion in Sec. 2.4), efficient and error-resistant entanglement distillations and connections, and complete optimizations of hybrid repeaters in comparison to their non-hybrid counterparts. Imperfections in the local repeater nodes as, for instance, in a CQED-based scheme might be circumvented through efficient free-space qubit-qumode interactions [228]. Similarly, the local CQED parts may also be highly improved through the use of microtoroidal cavities [229].

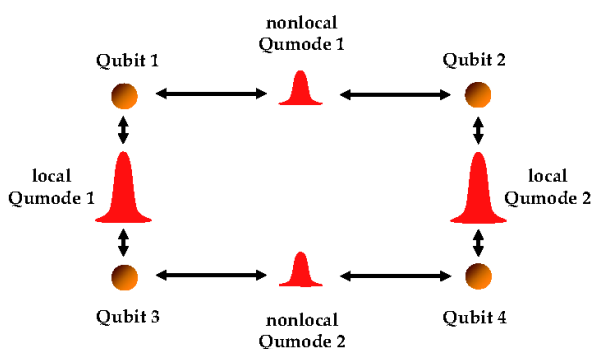


Figure: 3.4.4 A hybrid quantum repeater segment. The non-local qumodes travel through optical fibers and are subject to photon losses depending on the channel distance. Thus, error-free, non-Gaussian photon measurements may be used to eliminate measurement-based errors and maximize fidelities for sufficiently small, loss-resistant qumode amplitudes. The local qumode states, however, may have large photon numbers, as their photon losses are independent of the communication distance (neglecting local coupling inefficiencies and dissipations during the light-matter interactions). Therefore the local qumode states can be well discriminated through homodyne detection, allowing for efficient implementations of local two-qubit operations necessary for entanglement distillation. Alternatively, the measurement-free sequences from Sec. 3.3.5 could be used for the local entangling gates.

Let us finally mention that there are indeed proposals for entanglement distillation that could be incorporated into a full hybrid quantum repeater. Since the flying quantum systems sent along the communication channel are photonic qumodes, such distillations may directly act upon these qumodes, for instance, in an entanglement distributor (Fig. 3.2.2) rather than a qubus-based scheme. Besides those proposals listed in Sec. 3.1, there are other very recent ideas achieving nondeterministic, noiseless amplification [230,231] with the help of DV Fock-state ancillae and phase concentration through amplification of attenuated coherent-state qumodes utilizing thermal noise addition and photon subtraction [232].

4. Summary and outlook

Quantum information protocols can be formulated in terms of either discrete or continuous degrees of freedom. In optical implementations, the feasibility and the efficiency of a quantum information protocol, including its basic sub-routines such as state preparation, manipulation, and measurements, depend on the type of variables employed in the scheme. In particular, the use of continuous quantum variables leads to very efficient implementations. However, recent studies have revealed that approaches solely based upon Gaussian continuous-variable (CV) states and Gaussian operations are ultimately limited: universal quantum computation cannot be achieved in the Gaussian regime alone; also entanglement distillation, a fundamental subroutine in quantum communication, as well as more general forms of quantum error correction are impossible in the realm of Gaussian states and Gaussian operations.

A possible way to circumvent these restrictions while maintaining some of the advantages of the CV approach is to utilize both continuous and discrete variables at the same time. For instance, entangled Gaussian cluster states, unconditionally producible from squeezed light sources, can still be used for universal quantum computation, provided a non-Gaussian measurement (e.g. through photon counting) is added to a cluster computation protocol. Similarly, a nonlinear interaction of cubic or higher order, otherwise hard to obtain on the level of single quanta, can be effectively enhanced when intense optical pulses in Gaussian states are used as a quantum bus to mediate qubit-qubit interactions. Such a scenario is particularly well suited to quantum communication schemes where discrete-variable (DV) quantum information is locally encoded into atomic qubit memories, but transmitted through an optical-fiber channel using a CV quantum bus.

We gave a (certainly incomplete) review over existing hybrid proposals for quantum information processing, including brief discussions of their underlying principles and the tools that they use. These hybrid schemes, based upon, for instance, linear resources, together with the exploitation of measurement-induced or weak nonlinearities, represent a promising route to efficient optical quantum computation and communication. They can be seen as part of the current effort to combine stable atomic and scalable solid-state systems for reliable storage and fast processing of quantum information with photonic systems for communication into hybrid devices.

The most attractive feature of those scheme in which the necessary nonlinear element for universal quantum information processing is solely provided through the measurement apparatus is that in this case the linear resource states such as Gaussian CV cluster states can be built in an efficient, unconditional fashion. Nonetheless, this unconditionality comes at a price: the finite squeezing of the qumodes within a cluster state leads to inevitable errors in a cluster computation. To suppress these errors, some form of efficient quantum error correction will be needed for which again a nonlinear element is required. The most

promising approach will be most likely based upon a combination of different encodings, resources, and measurement techniques, as envisaged by the hybrid schemes discussed in this review: photonic qubits universally processed on their own utilizing polarization dual-rail encoding and efficiently coupled with other qubits by employing nonlinearly transformed or measured Gaussian photonic qumode ancillae.

Acknowledgements I would like to thank the DFG for financial support through the Emmy Noether programme. Further I acknowledge useful inputs and assistance from Akira Furusawa, Norbert Lütkenhaus, Damian Markham, Nick Menicucci, Bill Munro, Kae Nemoto, and Tim Ralph.

References

- [1] R. Raussendorf and H. J. Briegel, *Phys. Rev. Lett.* **86**, 5188 (2001).
- [2] H. J. Briegel, W. Dür, J. I. Cirac and P. Zoller, *Phys. Rev. Lett.* **81**, 5932 (1998).
- [3] W. Dür, H. J. Briegel, J. I. Cirac and P. Zoller, *Phys. Rev. A* **59**, 169 (1999).
- [4] D. Bouwmeester, J.-W. Pan, K. Mattle, M. Eibl, H. Weinfurter and A. Zeilinger, *Nature* **390**, 575 (1997).
- [5] A. Furusawa, J. L. Sørensen, S. L. Braunstein, C. A. Fuchs, H. J. Kimble and E. S. Polzik, *Science* **282**, 706 (1998).
- [6] P. Kok, W. J. Munro, Kae Nemoto, T. C. Ralph, Jonathan P. Dowling, and G. J. Milburn, *Rev. Mod. Phys.* **79**, 135 (2007).
- [7] S. L. Braunstein and P. van Loock, *Rev. Mod. Phys.* **77**, 513-577 (2005).
- [8] S. Lloyd and S. L. Braunstein, *Phys. Rev. Lett.* **82**, 1784 (1999).
- [9] S. D. Bartlett, B. C. Sanders, S. L. Braunstein, and K. Nemoto, *Phys. Rev. Lett.* **88**, 097904 (2002).
- [10] D. Gottesman, A. Kitaev, and J. Preskill, *Phys. Rev. A* **64**, 012310 (2001).
- [11] E. Knill, R. Laflamme and G. J. Milburn, *Nature* **409**, 46 (2001).
- [12] N. Lütkenhaus, J. Calsamiglia, and K.A. Suominen, *Phys. Rev. A* **59**, 3295 (1999).
- [13] P. van Loock and N. Lütkenhaus, *Phys. Rev. A* **69**, 012302 (2004).
- [14] Ph. Raynal, P. van Loock, and N. Lütkenhaus, *Proceedings of the Seventh International Conference on Quantum Communication, Measurement and Computing QCMC 2004*, Glasgow, UK, p.91-95, American Institute of Physics, New York (2004).
- [15] P. Grangier, J. A. Levenson, and J. P. Poizat, *Nature* **396**, 537 (1998).
- [16] M. G. A. Paris, M. Plenio, D. Jonathan, S. Bose, and G. M. D'Ariano, *Phys. Lett. A* **273**, 153 (2000).
- [17] K. Nemoto and W. J. Munro, *Phys. Rev. Lett.* **93**, 250502 (2004).
- [18] S. D. Barrett, P. Kok, Kae Nemoto, R. G. Beausoleil, W. J. Munro, and T. P. Spiller, *Phys. Rev. A* **71**, 060302 (2005).
- [19] W. J. Munro, K. Nemoto, R. G. Beausoleil, and T. P. Spiller, *Phys. Rev. A* **71**, 033819 (2005).
- [20] W. J. Munro, K. Nemoto, and T. P. Spiller, *New J. Phys.* **7**, 137 (2005).
- [21] T. P. Spiller, K. Nemoto, S. L. Braunstein, W. J. Munro, P. van Loock, and G. J. Milburn, *New J. Phys.* **8**, 30 (2006).
- [22] P. van Loock, W. J. Munro, Kae Nemoto, T. P. Spiller, T. D. Ladd, S. L. Braunstein, G. J. Milburn, *Phys. Rev. A* **78**, 022303 (2008).
- [23] D. F. Walls and G. J. Milburn, *Quantum Optics*, Springer Verlag Berlin Heidelberg New York (1994).
- [24] N. N. Bogoliubov, *J. Phys.* **11**, 23 (1947).
- [25] J. Yoshikawa, T. Hayashi, T. Akiyama, N. Takei, A. Huck, U.L. Andersen, and A. Furusawa, *Phys. Rev. A* **76**, 060301(R) (2007).
- [26] J. Yoshikawa, Y. Miwa, A. Huck, U. L. Andersen, P. van Loock, and A. Furusawa, *Phys. Rev. Lett.* **101**, 250501 (2008).
- [27] R. Filip, P. Marek, and U. L. Andersen, *Phys. Rev. A* **71**, 042308 (2005).
- [28] S. L. Braunstein, *Phys. Rev. A* **71**, 055801 (2005).
- [29] M. Reck, A. Zeilinger, H. J. Bernstein and P. Bertani, *Phys. Rev. Lett.* **73**, 58 (1994).
- [30] A. Ourjoumtsev *et al.*, *Science* **312**, 83 (2006).
- [31] J. S. Neergaard-Nielsen *et al.*, *Phys. Rev. Lett.* **97**, 083604 (2006).
- [32] H. Takahashi *et al.*, *Phys. Rev. Lett.* **101**, 233605 (2008).
- [33] K. Banaszek, *Phys. Lett. A* **253**, 12 (1999).
- [34] I. D. Ivanovic, *Phys. Lett. A* **123**, 257 (1987).
- [35] D. Dieks, *Phys. Lett. A* **126**, 303 (1988).
- [36] A. Peres, *Phys. Lett. A* **128**, 19 (1988).
- [37] S. J. van Enk, *Phys. Rev. A* **66**, 042313 (2002).
- [38] M. A. Nielsen and I. L. Chuang, *Quantum Computation and Quantum Information*, Cambridge University Press (2000).
- [39] N. J. Cerf, C. Adami, and P. G. Kwiat, *Phys. Rev. A* **57**, R1477 (1998).
- [40] P. G. Kwiat and H. Weinfurter, *Phys. Rev. A* **58**, R2623 (1998).
- [41] C. Schuck *et al.*, *Phys. Rev. Lett.* **96**, 190501 (2006).
- [42] M. Barbieri *et al.*, *Phys. Rev. A* **75**, 042317 (2007).
- [43] M. M. Wilde and D. B. Uskov, *Phys. Rev. A* **79**, 022305 (2008).
- [44] D. Gottesman and I. Chuang, *Nature* **402**, 390 (1999).
- [45] E. Knill, *Phys. Rev. A* **68**, 064303 (2003).
- [46] S. Scheel and N. Lütkenhaus, *New J. Phys.* **6**, 51 (2004).
- [47] J. Eisert, *Phys. Rev. Lett.* **95**, 040502 (2005).
- [48] D. B. Uskov *et al.*, *Phys. Rev. A* **79**, 042326 (2009).
- [49] J. L. O'Brien *et al.*, *Nature* **426**, 264 (2003).
- [50] A. S. Clark *et al.*, *Phys. Rev. A* **79**, 030303(R) (2009).
- [51] J. Calsamiglia and N. Lütkenhaus, *Appl. Phys. B* **72**, 67 (2001).
- [52] M. A. Nielsen, *Phys. Rev. Lett.* **93**, 040503 (2004).
- [53] D. E. Browne and T. Rudolph, *Phys. Rev. Lett.* **95**, 010501 (2005).
- [54] D. Gross, K. Kieling, and J. Eisert, *Phys. Rev. A* **74**, 042343 (2006).
- [55] K. Kieling, T. Rudolph, and J. Eisert, *Phys. Rev. Lett.* **99**, 130501 (2007).
- [56] N. C. Menicucci, P. van Loock, M. Gu, C. Weedbrook, T. C. Ralph, and M. A. Nielsen, *Phys. Rev. Lett.* **97**, 110501 (2006).
- [57] D. Boschi, S. Branca, F. De Martini, L. Hardy, and S. Popescu, *Phys. Rev. Lett.* **80**, 1121 (1998).

- [58] N. Gisin, *Nature Phys.* **1**, 165 (2007).
- [59] N. Gisin *et al.*, *Rev. Mod. Phys.* **74**, 145 (2002).
- [60] N. Lütkenhaus and A. J. Shields *eds.*, *Focus on Quantum Cryptography: Theory and Practice*, *New J. Phys.* **11**, 045005 (2009).
- [61] D. Stebila, M. Mosca, and N. Lütkenhaus, arXiv: 0902.2839 [quant-ph] (2009).
- [62] H. J. Kimble, *Nature* **453**, 1023 (2008).
- [63] W. K. Wootters and W. H. Zurek, *Nature* **299**, 802 (1982).
- [64] D. Dieks, *Physics Letters* **92A**, 271 (1982).
- [65] M. Zukowski, A. Zeilinger, M. A. Horne, and A. K. Ekert, *Phys. Rev. Lett.* **71**, 4287 (1993).
- [66] C. H. Bennett, G. Brassard, S. Popescu, B. Schumacher, J. A. Smolin, and W. K. Wootters, *Phys. Rev. Lett.* **76**, 722 (1996).
- [67] D. Deutsch, A. Ekert, R. Jozsa, C. Macchiavello, S. Popescu, and A. Sanpera, *Phys. Rev. Lett.* **77**, 2818 (1996).
- [68] B. C. Jacobs, T. B. Pittman, and J. D. Franson, *Phys. Rev. A* **66**, 052307 (2002).
- [69] H. de Riedmatten *et al.*, *Phys. Rev. Lett.* **92**, 047904 (2004).
- [70] A. Scherer *et al.*, *Phys. Rev. A* **80**, 062310 (2009).
- [71] L. Hartmann *et al.*, *Phys. Rev. A* **75**, 032310 (2007).
- [72] H. Aschauer, Ph.D. thesis, LMU Munich (2004); <http://edoc.ub.uni-muenchen.de/archive/00003588/>.
- [73] A. M. Tyryshkin *et al.*, *Phys. Rev. B* **68**, 193207 (2003).
- [74] R. Zhao *et al.*, *Nature Phys.* **5**, 100 (2008).
- [75] B. Zhao *et al.*, *Nature Phys.* **5**, 95 (2008).
- [76] J. J. L. Morton *et al.*, *Nature* **455**, 1085 (2008).
- [77] T. D. Ladd *et al.*, *Phys. Rev. B* **71**, 014401 (2005).
- [78] D. Stucki *et al.*, *New J. Phys.* **11**, 075003 (2009).
- [79] T. Scheidl *et al.*, *New J. Phys.* **11**, 085002 (2009).
- [80] L. Childress, J. M. Taylor, A. S. Sørensen, and M. D. Lukin, *Phys. Rev. Lett.* **96**, 070504 (2006).
- [81] L. Childress, J. M. Taylor, A. S. Sørensen, and M. D. Lukin, *Phys. Rev. A* **72**, 052330 (2005).
- [82] L. M. Duan, M. D. Lukin, J. I. Cirac, and P. Zoller, *Nature* **414**, 413 (2001).
- [83] C. Simon *et al.*, *Phys. Rev. Lett.* **98**, 190503 (2007).
- [84] Bo Zhao *et al.*, *Phys. Rev. Lett.* **98**, 240502 (2007).
- [85] Z.-B. Chen *et al.*, *Phys. Rev. A* **76**, 022329 (2007).
- [86] L. Jiang, J. M. Taylor, and M. D. Lukin, *Phys. Rev. A* **76**, 012301 (2007).
- [87] C. W. Chou *et al.*, *Nature* **438**, 828 (2005).
- [88] T. Chaneliere *et al.*, *Nature* **438**, 833 (2005).
- [89] M. D. Eisaman *et al.*, *Nature* **438**, 837 (2005).
- [90] Y.-A. Chen *et al.*, *Nature Phys.* **4**, 103 (2008).
- [91] M. Razavi and J. H. Shapiro, *Phys. Rev. A* **73**, 042303 (2006).
- [92] J. F. Sherson *et al.*, *Nature* **443**, 557 (2006).
- [93] B. Julsgaard *et al.*, *Nature* **432**, 482 (2004).
- [94] S. Tanzilli *et al.*, *Nature* **437**, 416 (2005).
- [95] M. Razavi, M. Piani, and N. Lütkenhaus, *Phys. Rev. A* **80**, 032301 (2009).
- [96] O. A. Collins *et al.*, *Phys. Rev. Lett.* **98**, 060502 (2007).
- [97] J. B. Brask and A. S. Sørensen, *Phys. Rev. A* **78**, 012350 (2008).
- [98] J. Eisert, S. Scheel, and M. B. Plenio, *Phys. Rev. Lett.* **89**, 137903 (2002).
- [99] J. Fiurášek, *Phys. Rev. Lett.* **89**, 137904 (2002).
- [100] G. Giedke and J. I. Cirac, *Phys. Rev. A* **66**, 032316 (2002).
- [101] M. Wallquist *et al.*, arXiv: 0911.3835 [quant-ph] (2009).
- [102] J. Niset, J. Fiurášek, and N. J. Cerf, *Phys. Rev. Lett.* **102**, 120501 (2009).
- [103] P. T. Cochrane, G. J. Milburn, and W. J. Munro, *Phys. Rev. A*, **62**, 062307 (2000).
- [104] N. J. Cerf *et al.*, *Phys. Rev. Lett.* **95**, 070501 (2005).
- [105] R. Demkowicz-Dobrzański, M. Kuś, and K. Wódkiewicz, *Phys. Rev. A* **69**, 012301 (2004).
- [106] C. Wittmann *et al.*, *Phys. Rev. Lett.* **101**, 210501 (2008).
- [107] A. I. Lvovsky, H. Hansen, T. Aichele, O. Benson, J. Mlynek, and S. Schiller, *Phys. Rev. Lett.* **87**, 050402 (2001).
- [108] M. Dakna, T. Anhut, T. Opatrný, L. Knöll, and D. G. Welsch, *Phys. Rev. A* **55**, 3184 (1997).
- [109] K. Wakui *et al.*, *Opt. Express* **15**, 3568 (2007).
- [110] A. M. Lance *et al.*, *Phys. Rev. A* **73**, 041801(R) (2006).
- [111] A. Ourjoumtsev *et al.*, *Nature* **448**, 784 (2007).
- [112] A. Zavatta, S. Viciani, and M. Bellini, *Science* **306**, 660 (2004).
- [113] V. Parigi *et al.*, *Science* **317**, 1890 (2007).
- [114] J. Fiurášek and N. J. Cerf, *Phys. Rev. Lett.* **93**, 063601 (2004).
- [115] K. Banaszek and K. Wódkiewicz, *Phys. Rev. A* **58**, 4345 (1998).
- [116] A. Ourjoumtsev *et al.*, *Phys. Rev. Lett.* **96**, 213601 (2006).
- [117] T. Opatrný, G. Kurizki, and D. G. Welsch, *Phys. Rev. A* **61**, 032302 (2000).
- [118] J. Eisert, D. E. Browne, S. Scheel, and M. B. Plenio, *Annals of Physics (NY)* **311**, 431 (2004).
- [119] L.-M. Duan, G. Giedke, J. I. Cirac, and P. Zoller, *Phys. Rev. Lett.* **84**, 4002 (2000).
- [120] L.-M. Duan, G. Giedke, J. I. Cirac, and P. Zoller, *Phys. Rev. A* **62**, 032304 (2000).
- [121] A. Ourjoumtsev *et al.*, *Phys. Rev. Lett.* **98**, 030502 (2007).
- [122] H. Takahashi *et al.*, arXiv: 0907.2159 [quant-ph] (2009).
- [123] B. Hage *et al.*, *Nature Phys.* **4**, 915 (2008).
- [124] R. Dong *et al.*, *Nature Phys.* **4**, 919 (2008).
- [125] S. Ghose and B. C. Sanders, *J. of Mod. Opt.* **54**, 855 (2007).
- [126] K. Nemoto and W. J. Munro, *Phys. Rev. Lett.* **93**, 250502 (2004).
- [127] S. L. Braunstein and H. J. Kimble, *Phys. Rev. Lett.* **80**, 869 (1998).
- [128] R. E. S. Polkinghorne and T. C. Ralph, *Phys. Rev. Lett.* **83**, 2095 (1999).
- [129] T. Ide *et al.*, *Phys. Rev. A* **65**, 012313 (2001).
- [130] T. Ide *et al.*, *Phys. Rev. A* **65**, 062303 (2002).
- [131] A. I. Lvovsky and M. G. Raymer, *Rev. Mod. Phys.* **81**, 299 (2009).
- [132] T. C. Ralph, E. H. Huntington, and T. Symul, *Phys. Rev. A* **77**, 063817 (2008).
- [133] A. Furusawa, private communication.
- [134] R. Filip, P. Marek, U. L. Andersen, *Phys. Rev. A* **71**, 042308 (2005).
- [135] P. K. Lam *et al.*, *Phys. Rev. Lett.* **79**, 1471 (1997).
- [136] P. van Loock, C. Weedbrook, and Mile Gu, *Phys. Rev. A* **76**, 032321 (2007).
- [137] M. Takeoka and M. Sasaki, *Phys. Rev. A* **78**, 022320 (2008).
- [138] C. W. Helstrom, *Quantum Detection and Estimation Theory*, New York Academic Press (1976).
- [139] M. Sasaki and O. Hirota, *Phys. Rev. A* **54**, 2728 (1996).
- [140] S. Dolinar, Research Laboratory of Electronics, MIT, Quarterly Progress Report **111** (1973), p. 115 (unpublished).

- [141] R. L. Cook, P. J. Martin, and J. M. Geremia, *Nature* **446**, 774 (2007).
- [142] A. P. Lund *et al.*, *Phys. Rev. Lett.* **100**, 030503 (2008), and Refs. therein.
- [143] C. M. Savage, S. L. Braunstein, and D. F. Walls, *Opt. Lett.* **15**, 628 (1990).
- [144] for example, W. P. Schleich, *Quantum Optics in Phase Space*, Wiley-VCH, Berlin (2001).
- [145] T. D. Ladd, P. van Loock, K. Nemoto, W. J. Munro, and Y. Yamamoto, *New J. Phys.* **8**, 184 (2006).
- [146] L.-M. Duan *et al.*, *Phys. Rev. Lett.* **84**, 2722 (2000).
- [147] R. Simon, *Phys. Rev. Lett.* **84**, 2726 (2000).
- [148] M. Horodecki, P. Horodecki, and R. Horodecki, *Phys. Lett. A* **223**, 1 (1996).
- [149] A. Peres, *Phys. Rev. Lett.* **77**, 1413 (1996).
- [150] E. Shchukin and W. Vogel, *Phys. Rev. Lett.* **95**, 230502 (2005).
- [151] A. Miranowicz and M. Piani, *Phys. Rev. Lett.* **97**, 058901 (2006).
- [152] W. Son *et al.*, *J. Mod. Opt.* **49**, 1739 (2002).
- [153] B. Kraus and J. I. Cirac, *Phys. Rev. Lett.* **92**, 013602 (2004).
- [154] X. Wang, *J. Phys. A: Math. Gen.* **35**, 165 (2002).
- [155] S. J. van Enk and O. Hirota, *Phys. Rev. A* **64**, 022313 (2001).
- [156] O. Hirota and M. Sasaki, arXiv: 0101018 [quant-ph] (2001).
- [157] M. Mehmet *et al.*, *Phys. Rev. A* **81**, 013814 (2010).
- [158] H. Vahlbruch *et al.*, *Phys. Rev. Lett.* **100**, 033602 (2008).
- [159] Y. Takeno *et al.*, *Opt. Express* **15**, 4321 (2007).
- [160] P. van Loock *et al.*, *Phys. Rev. A* **78**, 062319 (2008).
- [161] J. Eisert and M. B. Plenio, *Int. J. Quant. Inf.* **1**, 479 (2003).
- [162] G. Adesso and F. Illuminati, *J. Phys. A* **40**, 7821 (2007).
- [163] M. M. Wolf, G. Giedke, and J. I. Cirac, *Phys. Rev. Lett.* **96**, 080502 (2006).
- [164] S. J. van Enk and O. Hirota, *Phys. Rev. A* **71**, 062322 (2005).
- [165] H. Häselser, T. Moroder, and N. Lütkenhaus, *Phys. Rev. A* **77**, 032303 (2008).
- [166] J. Rigas, O. Gühne, and N. Lütkenhaus, *Phys. Rev. A* **73**, 012341 (2006).
- [167] C. Wittmann *et al.*, arXiv: 0911.3032 [quant-ph] (2009).
- [168] M. Curty, M. Lewenstein, and N. Lütkenhaus, *Phys. Rev. Lett.* **92**, 217903 (2004).
- [169] R. M. Gomes *et al.*, *PNAS* **106**, 21517 (2009).
- [170] S. J. van Enk, *Phys. Rev. A* **60**, 5095 (1999).
- [171] T. Aoki *et al.*, *Nature Phys.* **5**, 541 (2009).
- [172] W. Son *et al.*, *J. Mod. Opt.* **49**, 1739 (2002).
- [173] B. Kraus and J. I. Cirac, *Phys. Rev. Lett.* **92**, 013602 (2004).
- [174] M. Paternostro, W. Son, and M. S. Kim, *Phys. Rev. Lett.* **92**, 197901 (2004).
- [175] Q. A. Turchette *et al.*, *Phys. Rev. A* **58**, 4056 (1998).
- [176] F. Benatti, R. Floreanini, and M. Piani, *Phys. Rev. Lett.* **91**, 070402 (2003).
- [177] D. Braun, *Phys. Rev. Lett.* **89**, 277901 (2002).
- [178] B. Reznik, *Found. Phys.* **33**, 167 (2003); arXiv: 0008006 [quant-ph] (2000).
- [179] A. Retzker, J. I. Cirac, and B. Reznik, *Phys. Rev. Lett.* **94**, 050504 (2005).
- [180] S. Lloyd, part I, chapter 5 in *Quantum Information with Continuous Variables*, eds. S. L. Braunstein and A. K. Pati, Kluwer Academic Publisher (2003); arXiv: 0008057 [quant-ph] (2000).
- [181] S. Glancy, H. M. Vasconcelos, and T. C. Ralph, *Phys. Rev. A* **70**, 022317 (2004).
- [182] G. A. Durkin *et al.*, *Phys. Rev. A* **70**, 062305 (2004).
- [183] S. Lloyd and J.-J.- Slotine, *Phys. Rev. Lett.* **80**, 4088 (1998).
- [184] S. L. Braunstein, *Phys. Rev. Lett.* **80**, 4084 (1998).
- [185] S. L. Braunstein, *Nature* **394**, 47 (1998).
- [186] P. van Loock, arXiv: 0811.3616 [quant-ph] (2008).
- [187] X. Wang and P. Zanardi, *Phys. Rev. A* **65**, 032327 (2002).
- [188] G. J. Milburn, arXiv: 9908037 [quant-ph] (1999).
- [189] K. Mølmer and A. Sørensen, *Phys. Rev. Lett.* **82**, 1835 (1999).
- [190] A. Sørensen and K. Mølmer, *Phys. Rev. A* **62**, 022311 (2000).
- [191] G. J. Milburn, S. Schneider, and D. F. V. James, *Fortschr. Phys.* **48**, 801 (2000).
- [192] T. P. Spiller, K. Nemoto, S. L. Braunstein, W. J. Munro, P. van Loock, and G. J. Milburn, *New J. Phys.* **8**, 30 (2006).
- [193] S. Lloyd, *Phys. Rev. Lett.* **75**, 346 (1995).
- [194] J. I. Cirac and P. Zoller, *Phys. Rev. Lett.* **74**, 4091 (1995).
- [195] A. Luis, *J. Phys. A* **34**, 7677 (2001).
- [196] M. Gu *et al.*, *Phys. Rev. A* **79**, 062318 (2009).
- [197] S. D. Bartlett and W. J. Munro, *Phys. Rev. Lett.* **90**, 117901 (2003).
- [198] H. F. Hofmann *et al.*, *Phys. Rev. A* **62**, 062304 (2000).
- [199] S. Glancy and E. Knill, *Phys. Rev. A* **73**, 012325 (2006).
- [200] S. Pirandola *et al.*, *Europhys. Lett.* **68**, 323 (2004).
- [201] P. Marek and J. Fiurášek, *Phys. Rev. A* **79**, 062321 (2009).
- [202] N. Jain *et al.*, arXiv: 0912.1552 [quant-ph] (2009).
- [203] P. van Loock, *J. Opt. Soc. Am. B* **24**, 340 (2007).
- [204] J. Zhang and S. L. Braunstein, *Phys. Rev. A* **73**, 032318 (2006).
- [205] R. Ukai *et al.*, arXiv: 0910.0660 [quant-ph] (2009).
- [206] N. C. Menicucci, S. T. Flammia, and O. Pfister, *Phys. Rev. Lett.* **101**, 130501 (2008).
- [207] N. C. Menicucci *et al.*, *Phys. Rev. A* **76**, 010302(R) (2007).
- [208] R. Ukai *et al.*, arXiv: 1001.4860 [quant-ph] (2010).
- [209] Y. Miwa *et al.*, *Phys. Rev. A* **80**, 050303(R) (2009).
- [210] M. Yukawa *et al.*, *Phys. Rev. A* **78**, 012301 (2008).
- [211] X. Su *et al.*, *Phys. Rev. Lett.* **98**, 070502 (2007).
- [212] G. Puentes *et al.*, arXiv: 0902.1549 [quant-ph] (2009).
- [213] S. G. R. Louis *et al.*, *New J. Phys.* **9**, 193 (2007).
- [214] S. G. R. Louis *et al.*, *Phys. Rev. A* **78**, 022326 (2008).
- [215] S. D. Barrett and G. J. Milburn, *Phys. Rev. A* **74**, 060302(R) (2006).
- [216] S. G. R. Louis *et al.*, *Phys. Rev. A* **75**, 042323 (2007).
- [217] J. I. Cirac, P. Zoller, H. J. Kimble, and H. Mabuchi, *Phys. Rev. Lett.* **78**, 3221 (1997).
- [218] S. Bose, P. L. Knight, M. B. Plenio and V. Vedral, *Phys. Rev. Lett.* **83**, 5158 (1999).
- [219] L.-M. Duan and H. J. Kimble, *Phys. Rev. Lett.* **90**, 253601 (2003).
- [220] D. Browne, M. B. Plenio, and S. Huelga, *Phys. Rev. Lett.* **91**, 067901 (2003).
- [221] Y. L. Lim, A. Beige, and L. C. Kwek, *Phys. Rev. Lett.* **95**, 030505 (2005).
- [222] S. D. Barrett and P. Kok, *Phys. Rev. A* **71**, 060310 (2005).

- [223] P. van Loock, T. D. Ladd, K. Sanaka, F. Yamaguchi, K. Nemoto, W. J. Munro, and Y. Yamamoto, Phys. Rev. Lett. **96**, 240501 (2006).
- [224] W. K. Wootters, Phys. Rev. Lett. **80**, 2245 (1998).
- [225] K. Azuma *et al.*, Phys. Rev. A **80**, 060303(R) (2009).
- [226] W. J. Munro *et al.*, Phys. Rev. Lett. **101**, 040502 (2008).
- [227] L. Praxmeyer and P. van Loock, arXiv: 0912.1522 [quant-ph] (2009).
- [228] M. Sondermann *et al.*, Appl. Phys. B **89**, 489 (2007).
- [229] T. Aoki *et al.*, Nature **443**, 671 (2006).
- [230] T. C. Ralph and A. P. Lund, arXiv: 0809.0326 [quant-ph] (2008).
- [231] F. Ferreyrol *et al.*, arXiv: 0912.2065 [quant-ph] (2009).
- [232] P. Marek and R. Filip, arXiv: 0907.2402 [quant-ph] (2009).